



US010610616B2

(12) **United States Patent**
Kheradvar et al.

(10) **Patent No.: US 10,610,616 B2**
(45) **Date of Patent: Apr. 7, 2020**

(54) **MESH ENCLOSED TISSUE CONSTRUCTS**

(71) Applicant: **The Regents of the University of California**, Oakland, CA (US)

(72) Inventors: **Arash Kheradvar**, Irvine, CA (US);
Samuel David Zuke, Irvine, CA (US)

(73) Assignee: **The Regents of the University of California**, Oakland, CA (US)

(*) Notice: Subject to any disclaimer, the term of this patent is extended or adjusted under 35 U.S.C. 154(b) by 205 days.

(21) Appl. No.: **15/725,241**

(22) Filed: **Oct. 4, 2017**

(65) **Prior Publication Data**

US 2018/0043058 A1 Feb. 15, 2018

Related U.S. Application Data

(63) Continuation-in-part of application No. 14/162,617, filed on Jan. 23, 2014, now Pat. No. 9,925,296, which is a continuation-in-part of application No. 13/427,807, filed on Mar. 22, 2012, now Pat. No. 8,936,650.

(60) Provisional application No. 61/756,451, filed on Jan. 24, 2013, provisional application No. 61/559,694, filed on Jan. 19, 2012, provisional application No. 61/540,330, filed on Sep. 28, 2011, provisional application No. 61/496,369, filed on Jun. 13, 2011, provisional application No. 61/466,882, filed on Mar. 23, 2011.

(51) **Int. Cl.**

A61L 27/38 (2006.01)
A61F 2/24 (2006.01)
A61L 27/56 (2006.01)
A61L 27/54 (2006.01)
D01F 6/70 (2006.01)
A61L 27/34 (2006.01)
A61L 27/04 (2006.01)
A61F 2/00 (2006.01)

(52) **U.S. Cl.**

CPC **A61L 27/3804** (2013.01); **A61F 2/24** (2013.01); **A61F 2/2412** (2013.01); **A61F 2/2415** (2013.01); **A61F 2/2418** (2013.01); **A61L 27/047** (2013.01); **A61L 27/34** (2013.01); **A61L 27/3808** (2013.01); **A61L 27/3826** (2013.01); **A61L 27/3886** (2013.01); **A61L 27/54** (2013.01); **A61L 27/56** (2013.01); **D01F 6/70** (2013.01); **A61F 2002/0086** (2013.01); **A61F 2250/0018** (2013.01); **A61L 2300/224** (2013.01); **A61L 2300/404** (2013.01); **A61L 2300/414** (2013.01); **A61L 2300/606** (2013.01); **A61L 2400/18** (2013.01); **A61L 2430/20** (2013.01)

(58) **Field of Classification Search**

CPC .. **A61L 27/3804**; **A61L 27/56**; **A61L 27/3826**; **A61L 27/3808**; **A61L 27/3886**; **A61L**

27/54; **A61L 2430/20**; **A61F 2/2415**; **A61F 2/2412**; **A61F 2/24**; **A61F 2/2418**; **A61F 2002/0086**; **A61F 2250/0018**
See application file for complete search history.

(56) **References Cited**

U.S. PATENT DOCUMENTS

4,191,218 A 3/1980 Clark et al.
6,103,255 A 8/2000 Levine et al.
6,139,575 A 10/2000 Shu et al.
6,337,198 B1 1/2002 Levene et al.
6,461,382 B1 10/2002 Cao
7,422,603 B2 9/2008 Lane
7,575,759 B2 8/2009 Murphy et al.
7,635,592 B2 12/2009 West et al.
7,846,728 B2 12/2010 Brooks et al.
7,871,435 B2 1/2011 Carpentier et al.
7,914,808 B2 3/2011 Malaviya et al.
7,968,026 B1 6/2011 Teoh et al.
7,972,377 B2 7/2011 Lane
8,017,396 B2 9/2011 Kumar et al.
8,039,258 B2 10/2011 Harris et al.
8,071,007 B1 12/2011 Teoh et al.
8,137,686 B2 3/2012 Kladakis et al.
2003/0027332 A1 2/2003 LaFrance et al.
2005/0002982 A1 1/2005 Mooney et al.
2005/0143810 A1 6/2005 Dauner et al.
2005/0181016 A1 8/2005 Freyman et al.
2006/0246584 A1 11/2006 Covelli
2006/0253192 A1 11/2006 Atala et al.
2007/0041952 A1 2/2007 Guilak et al.
2009/0163612 A1 6/2009 Brady et al.
2009/0252795 A1 10/2009 Smyth

(Continued)

FOREIGN PATENT DOCUMENTS

WO WO 00/42950 A2 7/2000

OTHER PUBLICATIONS

Zuke, Samuel David, Feasibility studies on using a thermoplastic polyurethane scaffold for hybrid tissue-engineered heart valves. Doctoral dissertation, UC Irvine, Sep. 2017. (Year: 2017).*
Chen et al., A novel approach via combination of electrospinning and FDM for tri-leaflet heart valve scaffold fabrication. *Frontiers of Materials Science in China*, vol. 3, No. 4 (Dec. 2009) pp. 359-366. (Year: 2009).*
Abu-Omar, Y. et al. 2008 "Prosthetic heart valves" *Surgery* 26: 496-500.

(Continued)

Primary Examiner — Kara D Johnson
(74) *Attorney, Agent, or Firm* — Knobbe, Martens, Olson & Bear, LLP

(57) **ABSTRACT**

A heart valve leaflet including a thermoplastic polyurethane (TPU) mesh material that has a stiffness that is comparable to a native heart valve leaflet, such that it functionally mimics a native heart valve leaflet. The heart valve leaflets optionally include one to three layers of cells cultured on each side of the mesh material. Also disclosed is a heart valve including the heart valve leaflet and a frame.

(56)

References Cited

U.S. PATENT DOCUMENTS

2010/0249922 A1 9/2010 Li et al.
2012/0015331 A1 1/2012 Wood et al.

OTHER PUBLICATIONS

- Aikawa, E. et al. 2006 "Human semilunar cardiac valve remodeling by activated cells from fetus to adult: Implications for postnatal adaptation, pathology and tissue engineering" *Circulation* 113: 1344-1352.
- Alavi, S.H. et al. 2011 "A hybrid self-regenerative tissue approach as a proper alternative for prosthetic heart valves" *ASAIO J* 57: 88.
- Alavi, H. et al. 2011 "A hybrid self-renewal engineered tissue for heart valve leaflets" Society of Heart Valve Disease, 6th Biennial Meeting (Abstract).
- Alavi, S.H. et al. 2012 "Metal mesh scaffold for tissue engineering of membranes" *Tissue Eng Part C* 18: 293-301.
- Adamczyk, M.M. et al. 2002 "Biaxial strain distributions in explanted porcine bioprosthetic valves" *J Heart Valve Dis* 11: 686-695.
- Appleton, A.J.E. et al. 2009 "Vascular smooth muscle cells as a valvular interstitial cell surrogate in heart valve tissue engineering" *Tissue Engineering Part A* 15: 3889-3897.
- Apte, S.S. et al. 2011 "Current developments in the tissue engineering of autologous heart valves: Moving towards clinical use" *Future Cardiology* 7: 77-97.
- Bobak, D. et al. 1986 "Characterization of clq receptor expression on human phagocytic cells: Effects of pdbu and fmip" *J Immunol* 136: 4604-4610.
- Boontheekul, T. et al. 2003 "Protein-based signaling systems in tissue engineering" *Current Opinion in Biotechnology* 14: 559-565.
- Boyan, B.D. et al. 1996 "Role of material surfaces in regulating bone and cartilage cell responses" *Biomaterials* 17: 137.
- Breuer, C.K. et al. 2004 "Application of tissue-engineering principles toward the development of semilunar heart valve substitute" *Tissue Engineering* 10: 1725-1736.
- Butcher, J.T. et al. 2006 "Profiles of valvular and vascular endothelial cells reveal phenotypic differences: influence of shear stress" *Arterioscler Thromb Vasc Biol* 26: 69-77.
- Chen, J. et al. 2009 "Spectroscopic characterization and microscopic imaging of extracted and in situ cutaneous collagen and elastic tissue components under two-photon excitation" *Skin Res Technol* 15: 416-426.
- Cox, G. et al. 2003 "3-Dimensional imaging of collagen using second harmonic generation" *J Struct Biol* 141: 53-62.
- D'Arcy, J.L. et al. 2011 "Valvular heart disease: The next cardiac epidemic" *Heart* 97: 91-93.
- Deymier-Black, A.C. et al. 2010 "Synchrotron x-ray diffraction study of load partitioning during elastic deformation of bovine dentin" *Acta Biomater* 6: 2172-2180.
- Ferrans, V.J. et al. 1978 "Structural changes in glutaraldehyde-treated porcine heterografts used as substitute cardiac valves: Transmission and scanning electron microscopic observations in 12 patients" *Am J Cardiol* 41: 1159-1184.
- Flanagan, T.C. et al. 2003 "Living artificial heart valve alternatives: A review" *Eur Cell Mater* 6: 28-45.
- Fong, P. et al. 2006 "The use of polymer based scaffolds in tissue-engineered heart valves" *Progress in Pediatric Cardiology* 21: 193-199.
- Gan, B.K. et al. 2007 "Comparison of protein surface attachment on untreated and plasma immersion ion implantation treated polystyrene: protein islands and carpet" *Langmuir* 23: 2741-2746.
- Georgiou, E. et al. 2000 "Second and third optical harmonic generation in type I collagen by nanosecond laser irradiation, over a broad spectral region" *Optics Communications* 176: 253-260.
- Grande-Allen, K. et al. 2011 "The heterogeneous biomechanics and mechanobiology of the mitral valve: implications for tissue engineering" *Current Cardiology Reports* 13: 113-120.
- Hahn, M.S. et al. 2007 "Physiologic pulsatile flow bioreactor conditioning of poly(ethylene glycol)-based tissue engineered vascular grafts" *Annals of Biomedical Engineering* 35: 190-200.
- Hara, M. et al. 2006 "Imaging pancreatic betacells in the intact pancreas" *Am J Physiol Endocrinol Metab* 290: E1041-1047.
- He et al. 2005 "Fabrication of collagen-coated biodegradable polymer nanofiber mesh and its potential for endothelial cells growth" *Biomaterials* 26(36): 7606-7615.
- Hildebrandt, J. et al. 1969 "Stress-strain relations of tissue sheets undergoing uniform two-dimensional stretch" *J Appl Physiol* 27: 758-762.
- Hoerstrup, S.P. et al. 2000 "Functional living trileaflet heart valves grown in vitro" *Circulation* 102: 111-44-49.
- Hoffmann, G. et al. 2008 "Durability of bioprosthetic cardiac valves" *Dtsch Arztebl Int* 105: 143-148.
- Hori, J. et al. 2003 "Neural progenitor cells lack immunogenicity and resist destruction as allografts" *Stem Cells* 21: 405-416.
- Iijima, K. et al. 2004 "Dissecting the pathological effects of human abeta40 and abeta42 in *drosophila*: A potential model for Alzheimer's Disease" *Proc Natl Acad Sci USA* 101: 6623-6628.
- Jansen, L.P. et al. 2004 "Surgical mesh as a scaffold for tissue regeneration in the esophagus" *European Surgical Research* 36: 104-111.
- Khaled, A. et al. 2002 "Cytokines and the control of lymphoid homeostasis" *Nat Rev Immunol* 2: 817-830.
- Kheradvar, A. et al. 2004 "Evaluation of isovolumic relaxation phase in the process of ventricular remodeling following myocardial infarction" *Engineering in Medicine and Biology Society (IEMBS) 26th Annual International conference of the IEEE* 2: 3654-3657.
- Kheradvar, A. et al. 2006 "Estimation of elastic and viscous properties of the left ventricle based on annulus plane harmonic behavior" *Conference Proceedings, Annual International Conference of the IEEE Engineering in Medicine and Biology Society*, p. 4.
- Kheradvar, A. et al. 2006 "An in vitro study of changing profile heights in mitral bioprostheses and their influence on flow" *ASAIO J* 52: 34-38.
- Kheradvar, A. et al. 2006 "Assessment of left ventricular viscoelastic components based on ventricular harmonic behavior" *Cardiovascular Engineering* 6: 30-39.
- Kheradvar, A. et al. 2009 "On mitral valve dynamics and its connection to early diastolic flow" *Annals of Biomedical Engineering* 37: 1-13.
- Kheradvar, A. et al. 2011 "A hybrid self-renewal engineered tissue for heart valve leaflets" *Society of Heart Valve Disease, 6th Biennial Meeting*.
- Kheradvar, A. et al. 2012 "The effects of dynamic saddle annulus and leaflet length on transmitral flow pattern and leaflet stress of a bioprosthetic mitral valve" *J Heart Valve Dis* 21(2): 225-233.
- Kieswener, K. et al. 1996 "Surface roughness modulates the local production of growth factors and cytokines by osteoblast-like mg-63 cells" *J Biomed Mater Res* 32: 55.
- Kondyurin, A. et al. 2008 "Calcium phosphate formation on plasma immersion ion implanted low density polyethylene and polytetrafluoroethylene surfaces" *J Materials Science: Materials in Medicine* 19: 1145-1153.
- Ku, C.H. et al. 2006 "Collagen synthesis by mesenchymal stem cells and aortic valve interstitial cells in response to mechanical stretch" *Cardiovasc Res* 71: 548-556.
- Kuznetsova, N. et al. 1998 "Sugars and polyols inhibit fibrillogenesis of type I collagen by disrupting hydrogen-bonded water bridges between the helices" *Biochemistry* 37: 11888-11895.
- Leitao, E. et al. 1998 "In vitro testing of surface-modified biomaterials" *J Materials Science: Materials in Medicine* 9: 543-548.
- Liu, Y.C. et al. 2003 "High-resolution confocal imaging and three-dimensional rendering" *Methods* 30: 86-93.
- Liu et al. 2004 "Surface modification of titanium, titanium alloys and related materials for biomedical applications" *Materials Science and Engineering R* 47: 49-121.
- Liu, A.C. et al. 2007 "The emerging role of valve interstitial cell phenotypes in regulating heart valve pathobiology" *Am J Pathol* 171: 1407-1418.
- Liu, W.F. et al. 2011 "Real-time in vivo detection of biomaterial-induced reactive oxygen species" *Biomaterials* 32: 1796-1801.
- Long, J. et al. 2003 "Elastic fiber production in cardiovascular tissue-equivalents" *Matrix Biology* 22: 339-350.

(56)

References Cited

OTHER PUBLICATIONS

- Ma, M. et al. 2011 "Development of cationic polymer coatings to regulate foreign-body responses" *Advanced Materials* 23: H189-H194.
- Maitz, M.F. et al. 2002 "Ion beam treatment of titanium surfaces for enhancing deposition of hydroxyapatite from solution" *Biomolecular Engineering* 19: 269-272.
- McGuigan, A.P. et al. 2008 "The thrombogenicity of human umbilical vein endothelial cell seeded collagen modules" *Biomaterials* 29: 2453-2463.
- Mendelson, K. et al. 2006 "Heart valve tissue engineering: Concepts, approaches, progress and challenges" *Annals of Biomedical Engineering* 34: 1799-1619.
- Misfeld et al. 2007 "Heart valve macro- and microstructure" *Phil Trans R Soc B* 362: 1421-1436.
- Mulholland, D.L. et al. 1996 "Cell biology of valvular interstitial cells" *Can J Cardiol* 12: 231-236.
- Na, G.C. et al. 1986 "In vitro collagen fibril assembly in glycerol solution: evidence for a helical cooperative mechanism involving microfibrils" *Biochemistry* 25: 958-966.
- Nkomo, V.T. et al. 2006 "Burden of valvular heart diseases: A population-based study" *Lancet* 368: 1005-1011.
- Oshida, Y. et al. 1993 "Effects of shot-peening on surface contact angles of biomaterials" *J Materials Science: Materials in Medicine* 4: 443-447.
- Pignataro, B. et al. 1997 "Improved cell adhesion to ion beam-irradiated polymer surfaces" *Biomaterials* 18: 1461-1470.
- Pypen, C.M.J.M. 1997 "Characterization of microblasted and reactive ion etched surfaces on the commercially pure metals niobium, tantalum, and titanium" *J Materials Science: Materials in Medicine* 6: 781-784.
- Rabkin-Aikawa, E. et al. 2004 "Dynamic and reversible changes of interstitial cell phenotype during remodeling of cardiac valves" *J Heart Valve Dis* 13: 841-847.
- Rabkin-Aikawa, E. et al. 2005 "Cardiovascular tissue engineering" *Cardiovascular Pathology* 11: 305-317.
- Rabkin-Aikawa, E. et al. 2005 "Heart valve regeneration" *Adv Biochem Eng Biotechnol* 94: 141-179.
- Sacks, M.S. et al. 2009 "Bioengineering challenges for heart valve tissue engineering" *Annual Rev of Biomed Engineering* 11: 289-313.
- Saidi, I.S. et al. 1995 "Mie and rayleigh modeling of visible-light scattering in neonatal skin" *Appl Opt* 34: 7410-7418.
- Salvador-Morales, C. et al. 2009 "Immunocompatibility properties of lipid-polymer hybrid nanoparticles with heterogeneous surface functional groups" *Biomaterials* 30: 2231-2240.
- Schenke-Layland, K. et al. 2006 Impact of cryopreservation on extracellular matrix structures of heart valve leaflets *Ann Thorac Surg* 81: 918-926.
- Schenke-Layland, K. et al. 2008 Non-invasive multiphoton imaging of extracellular matrix structures: *J Biophotonics* 1: 451-462.
- Shah, S.R. V.N. 2008 "The effect of glycosaminoglycan stabilization on tissue buckling in bioprosthetic heart valves" *Biomaterials* 29: 1645-1653.
- Shenton, M.J. et al. 2005 "Ultralow energy ion beam surface modification of low density polyethylene" *J Physical Chem B* 109: 22185-22088.
- Shinoka, T. et al. 1995 "Tissue engineering heart valves: Valve leaflet replacement study in a lamb model" *Ann Thorac Surg* 60: S513-516.
- Shinoka, T. et al. 1996 "Tissue-engineered heart valves: Autologous valve leaflet replacement study in a lamb model" *Circulation* 94: 164-168.
- Smith, D.B. et al. 1999 "Fatigue-induced changes in bioprosthetic heart valve three dimensional geometry and the relation to tissue damage" *J Heart Valve Dis* 8: 25-33.
- Steinhoff, G. et al. 2000 "Tissue engineering of pulmonary heart valves on allogenic acellular matrix conduits: in vivo restoration of valve tissue" *Circulation* 102:111-50-55.
- Stephens, E.H. et al. 2010 "Age-related changes in material behavior of porcine mitral and aortic valves and correlation to matrix composition" *Tissue Engineering Part A* 16: 867-878.
- Sugita, Y. et al. 2009 "Experimental evaluation of a new antithrombogenic stent using ion beam surface modification" *Artificial Organs* 33: 456-463.
- Syedain, Z.H. et al. 2009 "Controlled cyclic stretch bioreactor for tissue-engineered heart valves" *Biomaterials* 30: 4078-4084.
- Tedder, M.E. et al. 2010 "Assembly and testing of stem cells-seeded layered collagen constructs for heart valve tissue engineering" *Tissue Eng Part A* 17: 25-36.
- Thubrikar, M. et al. 1983 "Role of mechanical stress in calcification of aortic bioprosthetic valves" *J Thorac Cardiovasc Surg* 86: 115-125.
- Tranquillo, Z.H. 2009 "Controlled cyclic stretch bioreactor for tissue-engineered heart valves" *Biomaterials* 30: 4078-4084.
- Trepanier, C. et al. 2000 "Corrosion Resistance and Biocompatibility of Passivated Nitinol" in *Shape Memory Implants* (ed.) L'H. Yahia, ndc, pp. 35-45.
- Van Den Broek, C.N. et al. 2008 "Medium with blood-analog mechanical properties for cardiovascular tissue culturing" *Biorheology* 45: 651-661.
- Van Der Merwe et al. 2008 "A computational study of knitted Nitinol meshes for their prospective use as external vein reinforcement" *J Biomechanics* 41: 1302-1309.
- Van Geemen, D. et al. 2011 "Decreased mechanical properties of heart valve tissue properties of heart valve tissue constructs cultured in platelet lysate as compared to fetal bovine serum" *Tissue Engineering Part C Methods* 17: 607-617.
- Vesely, I. et al. 1988 "Tissue buckling as a mechanism of bioprosthetic valve failure" *Ann Thorac Surg* 46: 302-308.
- Vesely, I. et al. 2001 "Tissue damage and calcification may be independent mechanisms of bioprosthetic heart valve failure" *J Heart Valve Dis* 10: 471-477.
- Vesely, I. 2005 "Heart valve tissue engineering" *Circ Res* 97: 743-755.
- Walachova, K. et al. 2002 "Colonization of ion-modified polyethylene with vascular smooth muscle cells in vitro" *Biomaterials* 23: 2989-2996.
- Wells, P.B. et al. 2006 "Influence of glycerol on the mechanical reversibility and thermal damage susceptibility of collagenous tissues" *IEEE Trans Biomed Eng* 53: 747-753.
- Wirrig, E.E. et al. 2011 "Differential expression of cartilage and bone-related proteins in pediatric and adult diseased aortic valves" *J Molec and Cell Cardiology* 50: 561-569.
- Wise et al. 2012 "Extracellular Matrix Molecules Facilitating Vascular Biointegration" *J Funct Biomater* 3(3): 569-587.
- Yee et al. 2009 "Enhancement of mesenchymal stem cell attachment to decellularized porcine aortic valve scaffold by in vitro coating with antibody against CD90: a preliminary study on antibody-modified tissue-engineered heart valve" *Tissue Eng Part A* 15(1): 1-11.
- Yeh, A.T. et al. 2003 "Reversible dissociation of collagen in tissues" *J Invest Dermatol* 121: 1332-1335.
- Zioupou, P. et al. 1992 "Mechanical and optical anisotropy of bovine pericardium" *Med Biol Eng Comput* 30: 76-82.
- Zund, G. et al. 1998 "Tissue engineering: A new approach in cardiovascular surgery; Seeding of human fibroblasts followed by human endothelial cells on resorbable mesh" *European Journal of Cardio-thoracic Surgery* 13: 160-164.

* cited by examiner

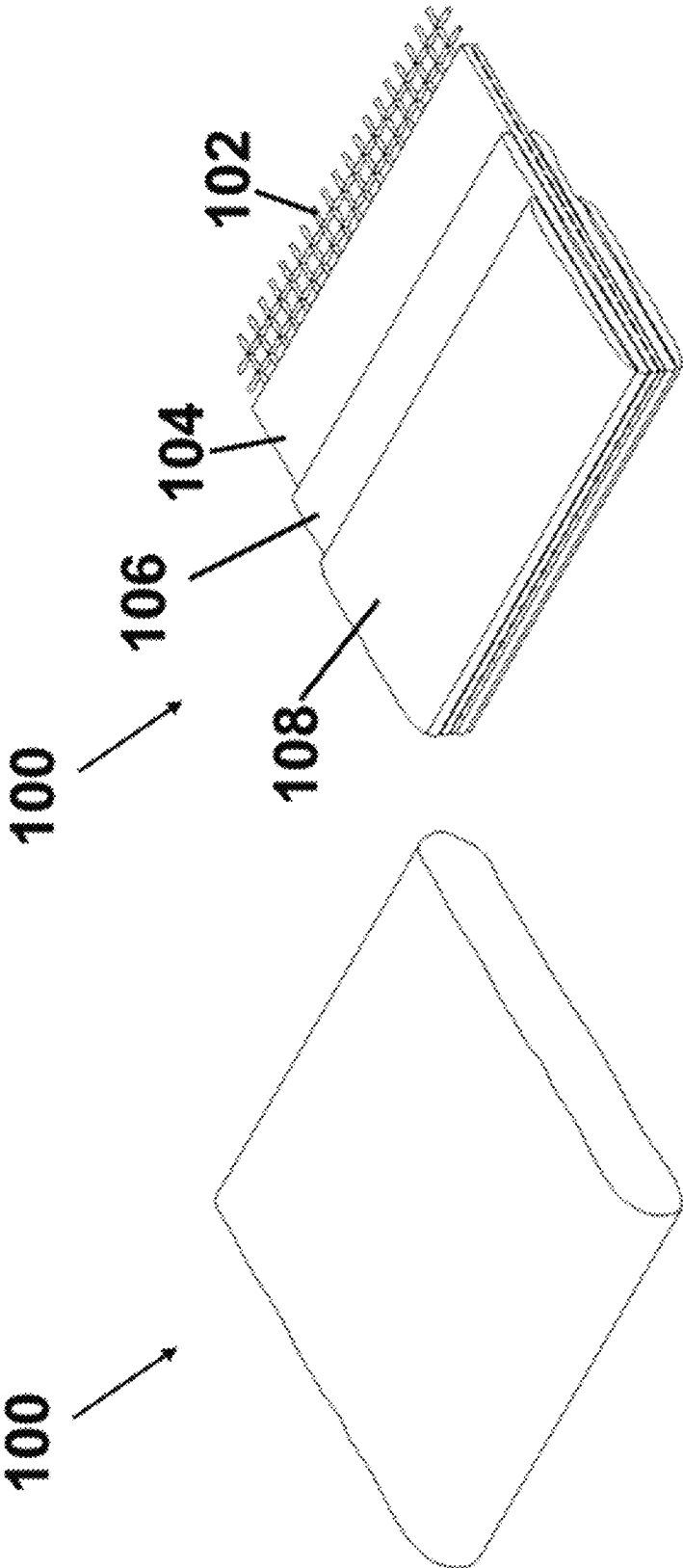


FIG. 1B

FIG. 1A

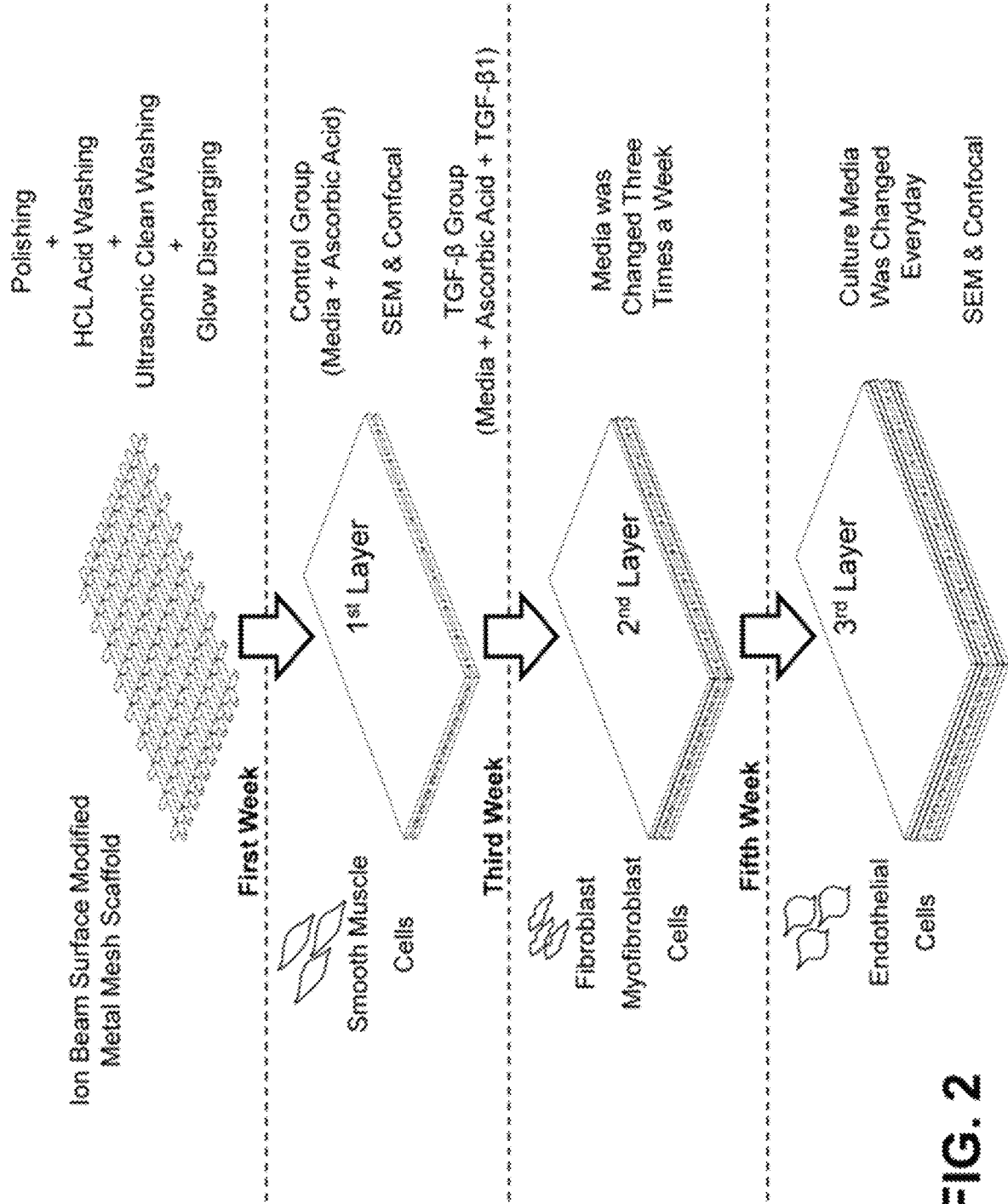


FIG. 2

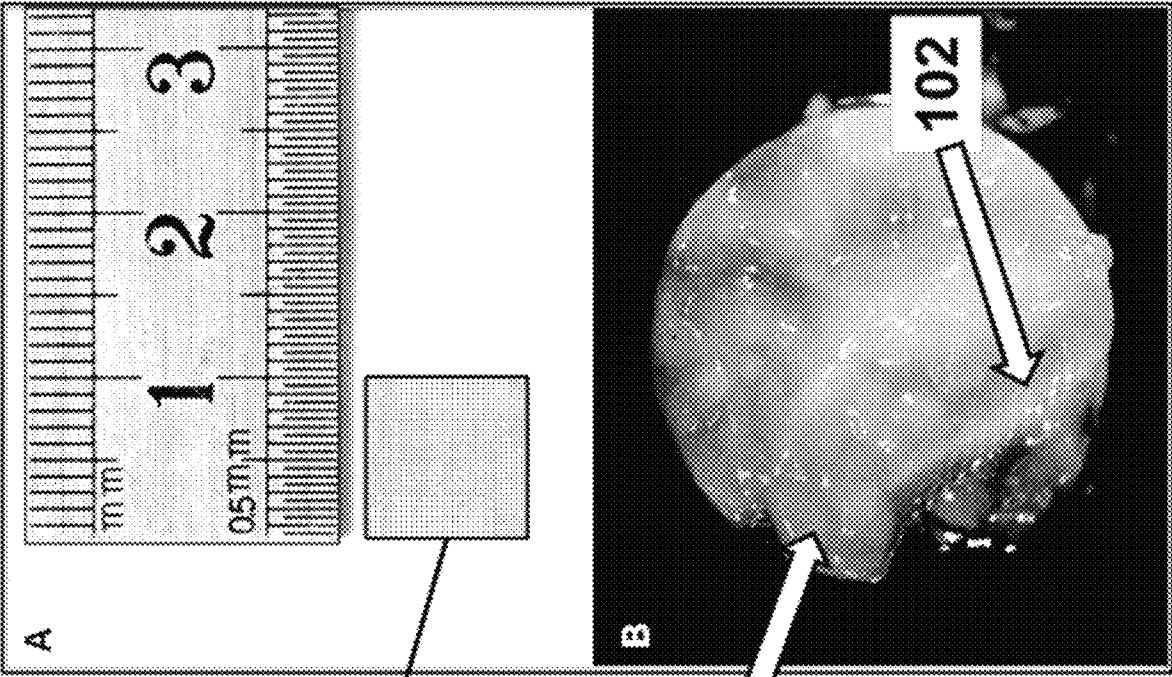


FIG. 3A

102

100

FIG. 3B

102

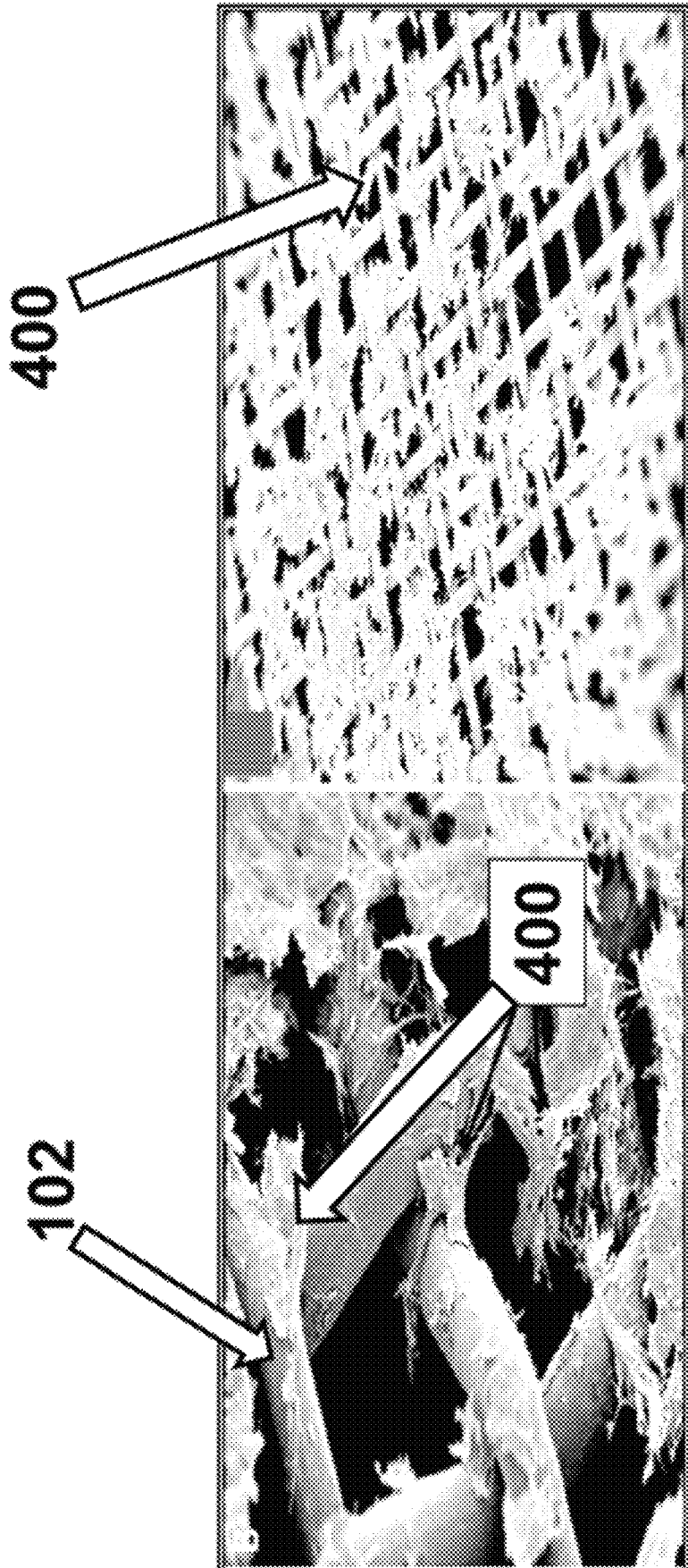


FIG. 4B

FIG. 4A

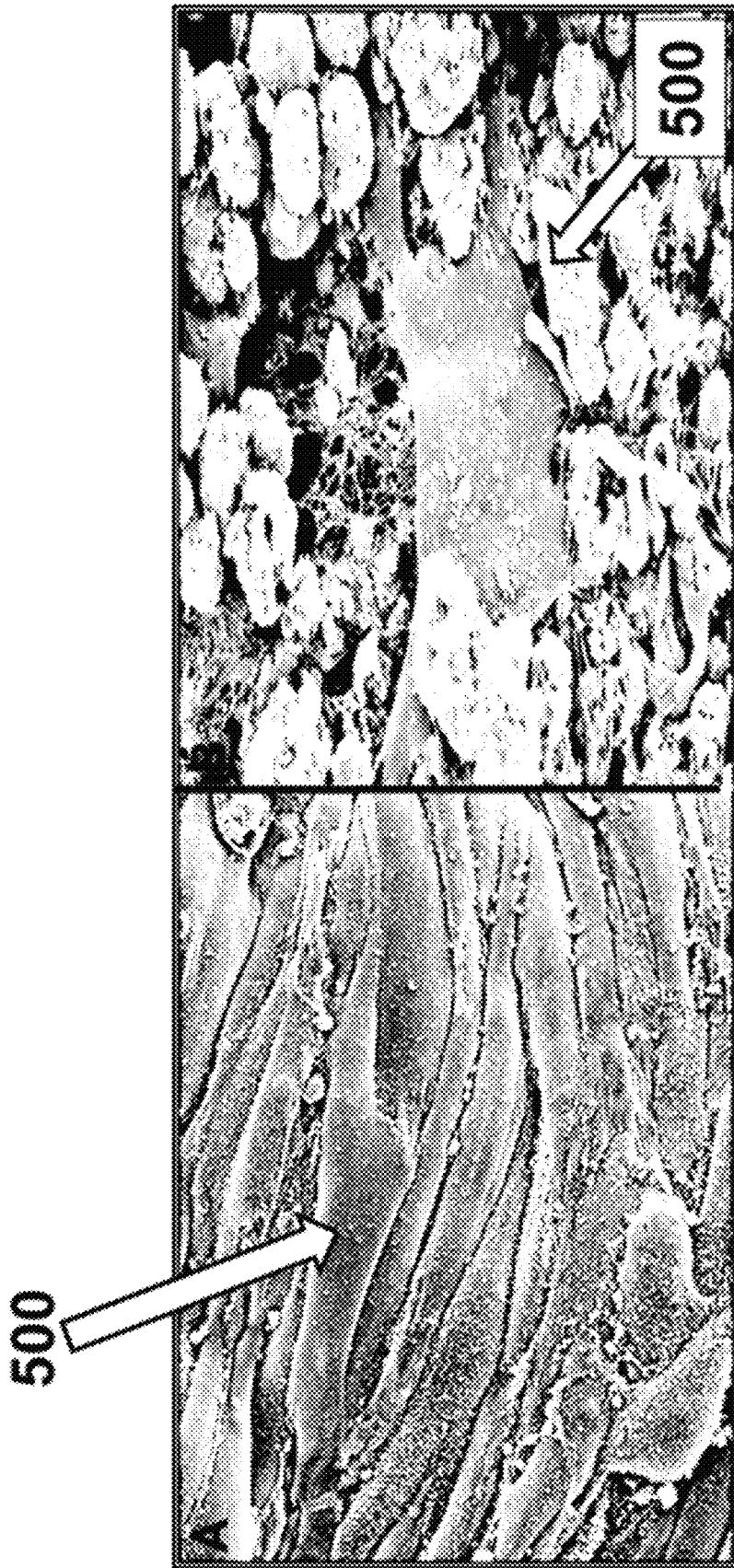


FIG. 5B

FIG. 5A

FIG. 6B

FIG. 6D

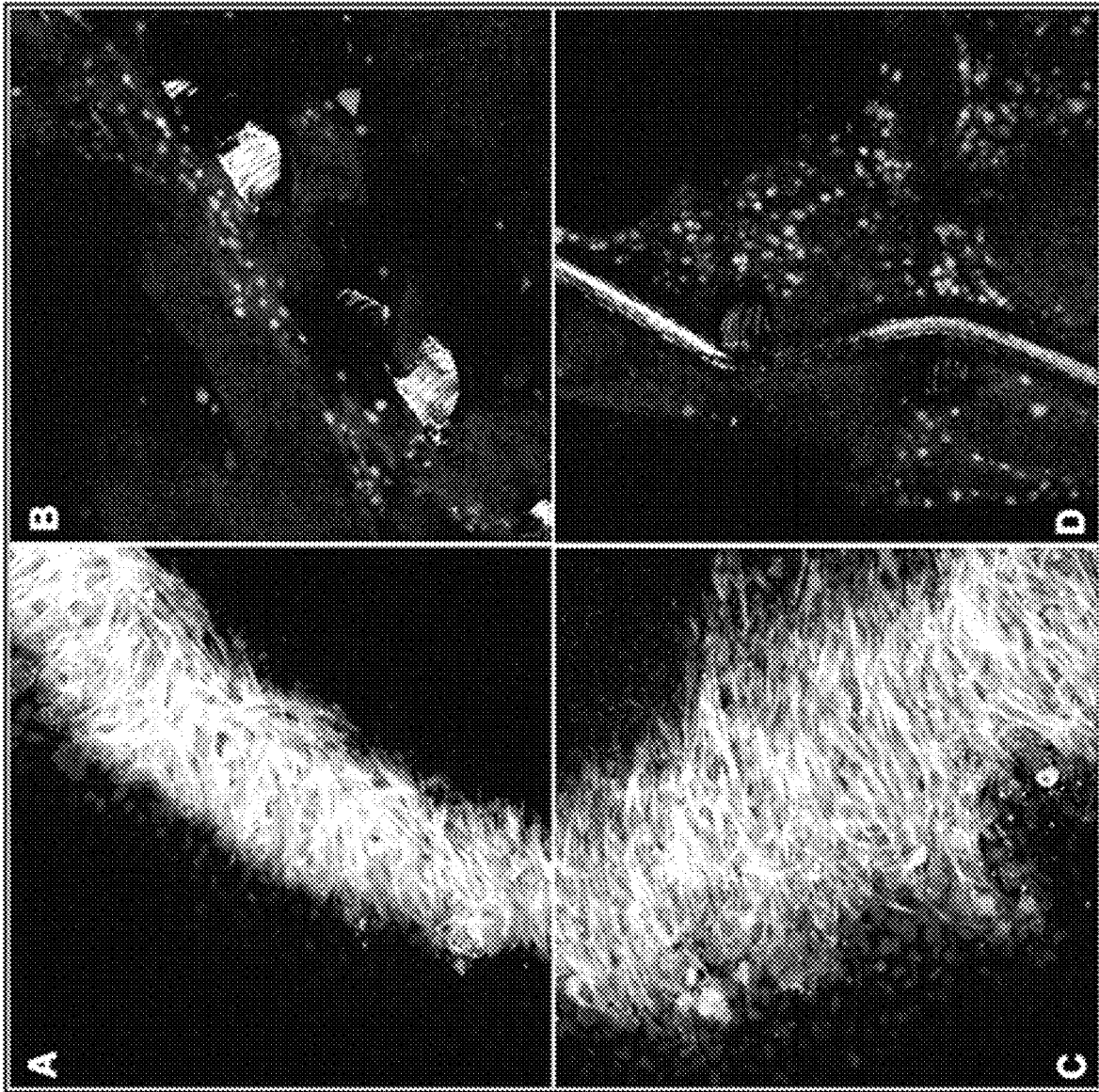
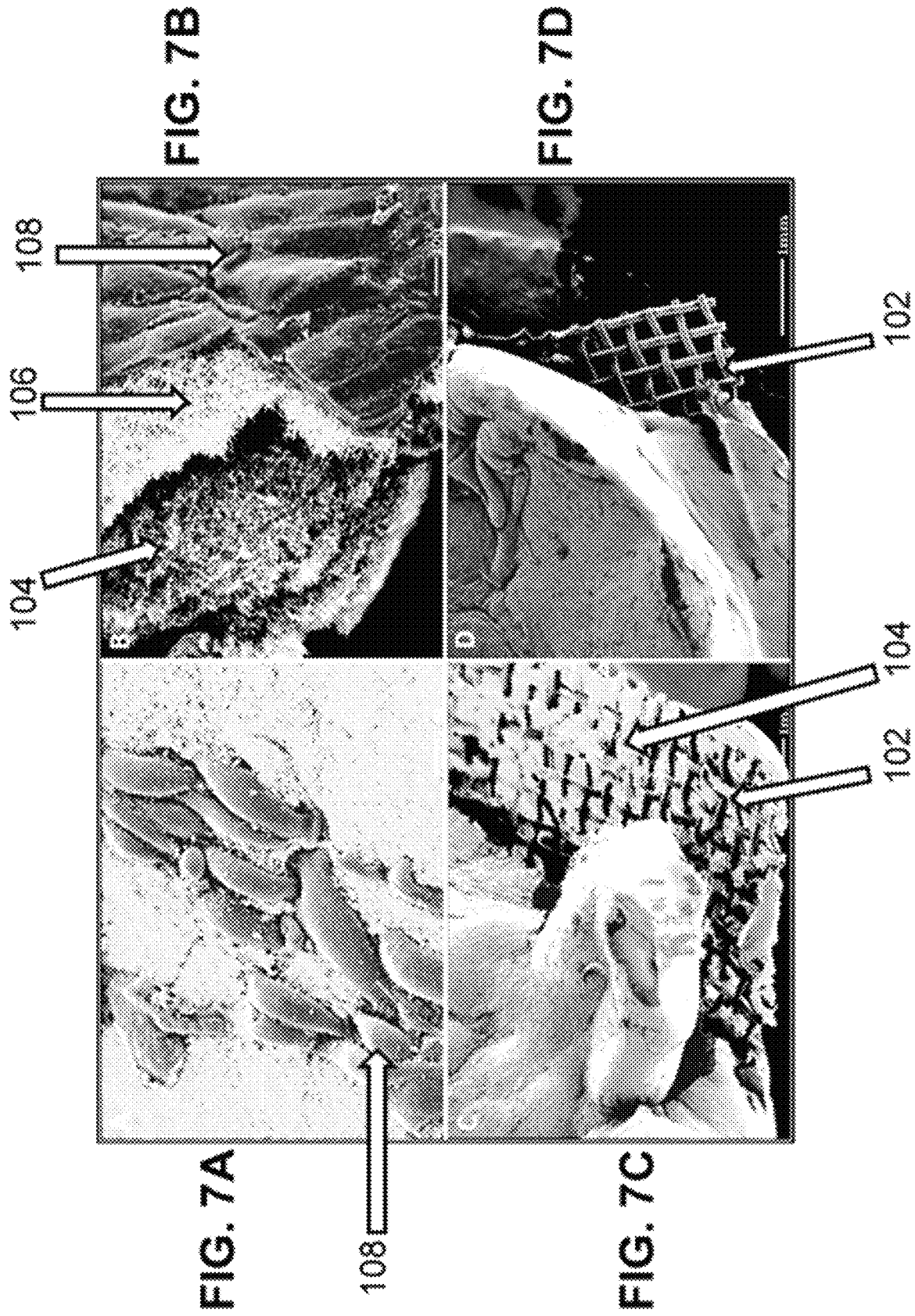


FIG. 6A

FIG. 6C



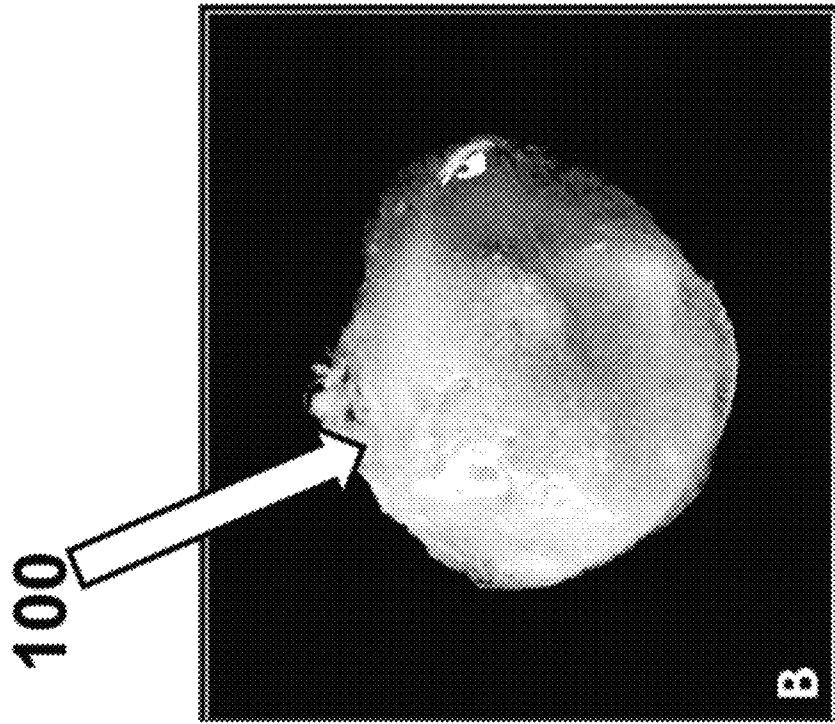


FIG. 8B

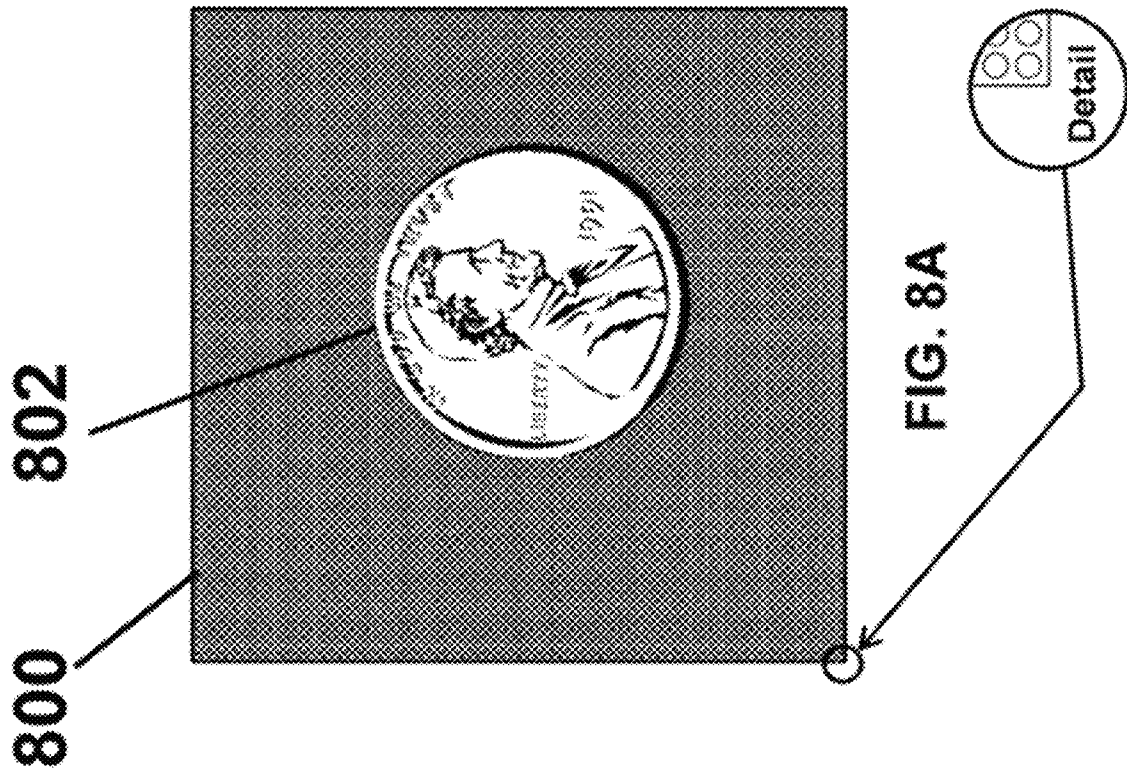
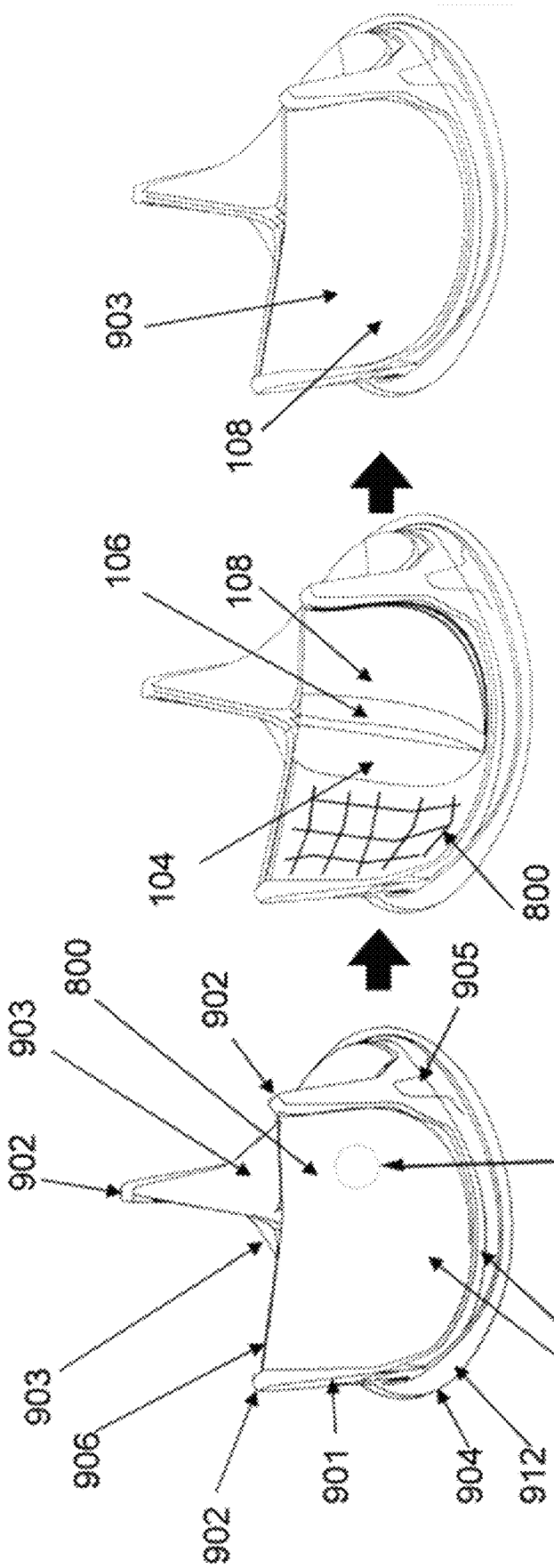


FIG. 8A



Detail Scale: 20:1

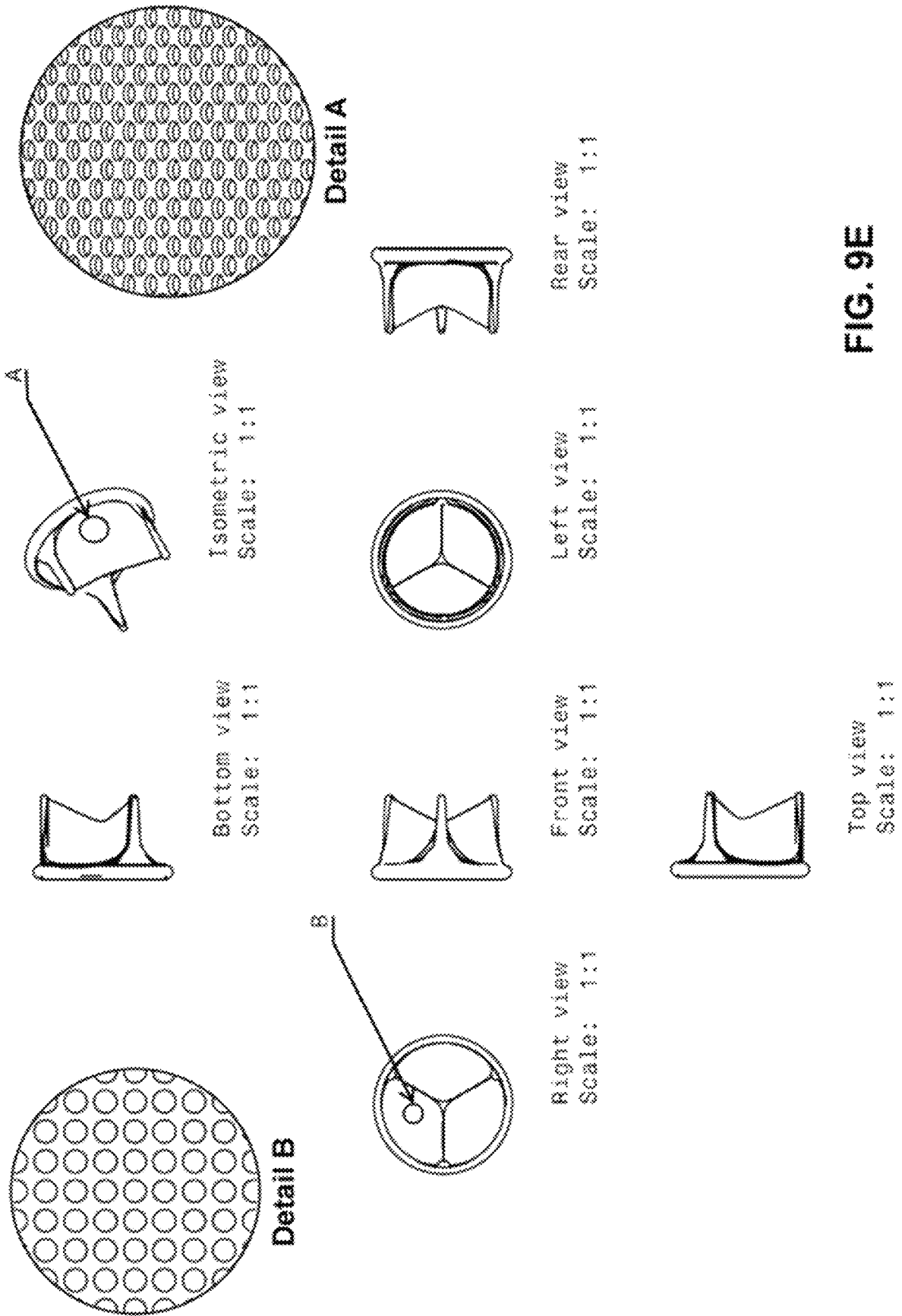


FIG. 9E

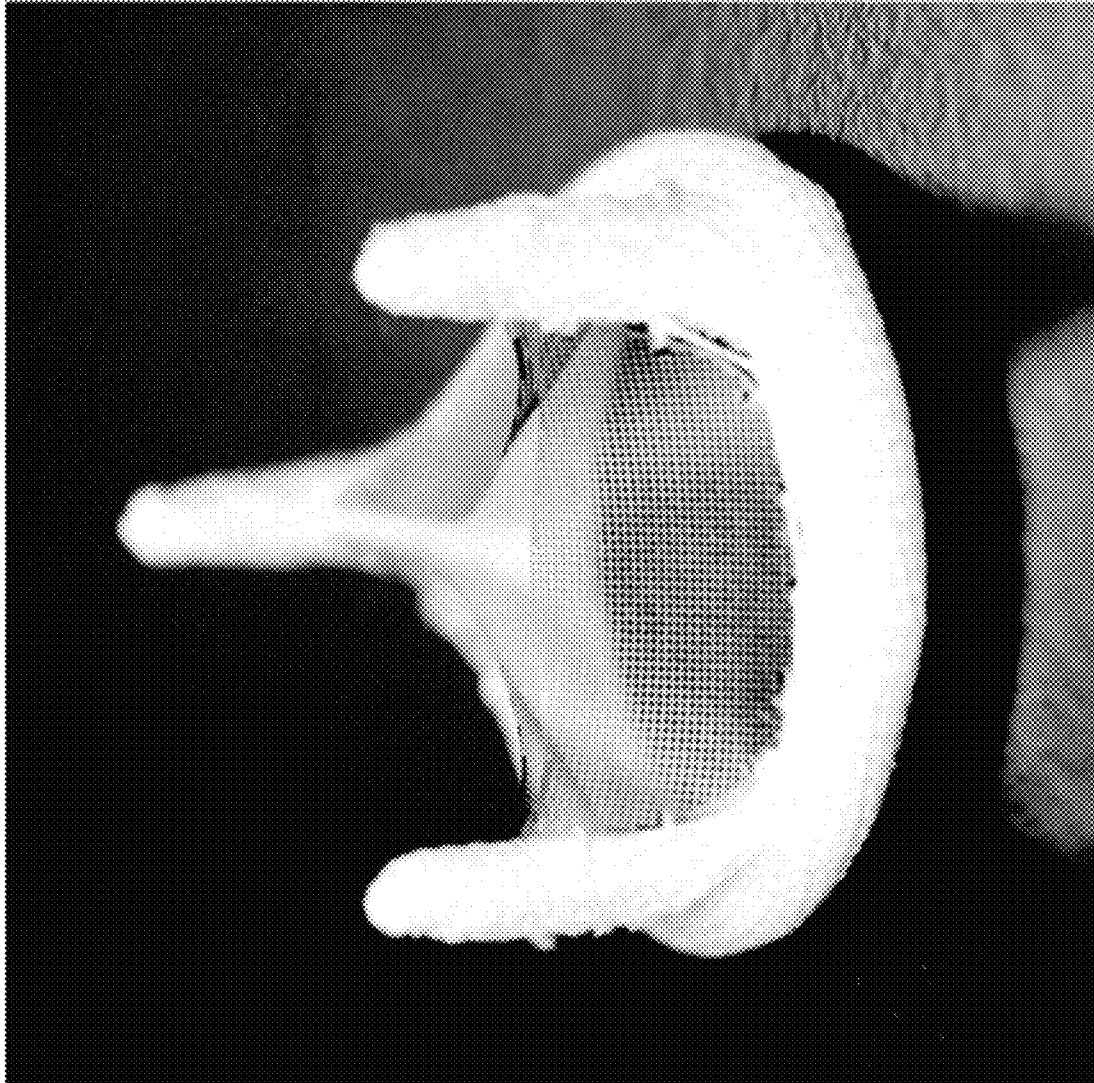


FIG. 9F

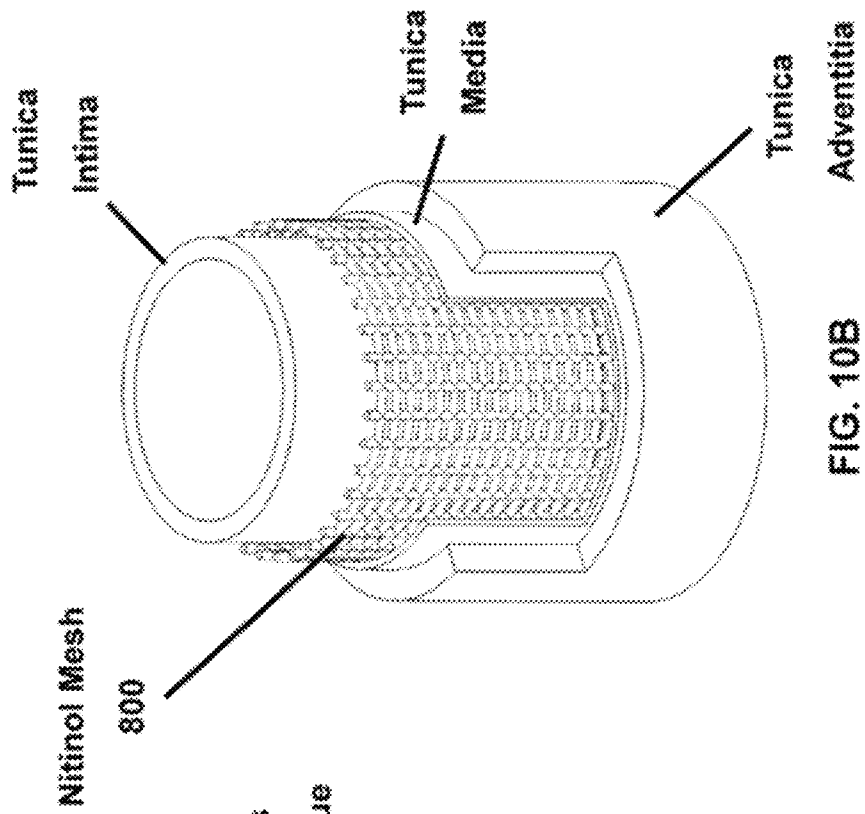


FIG. 10A

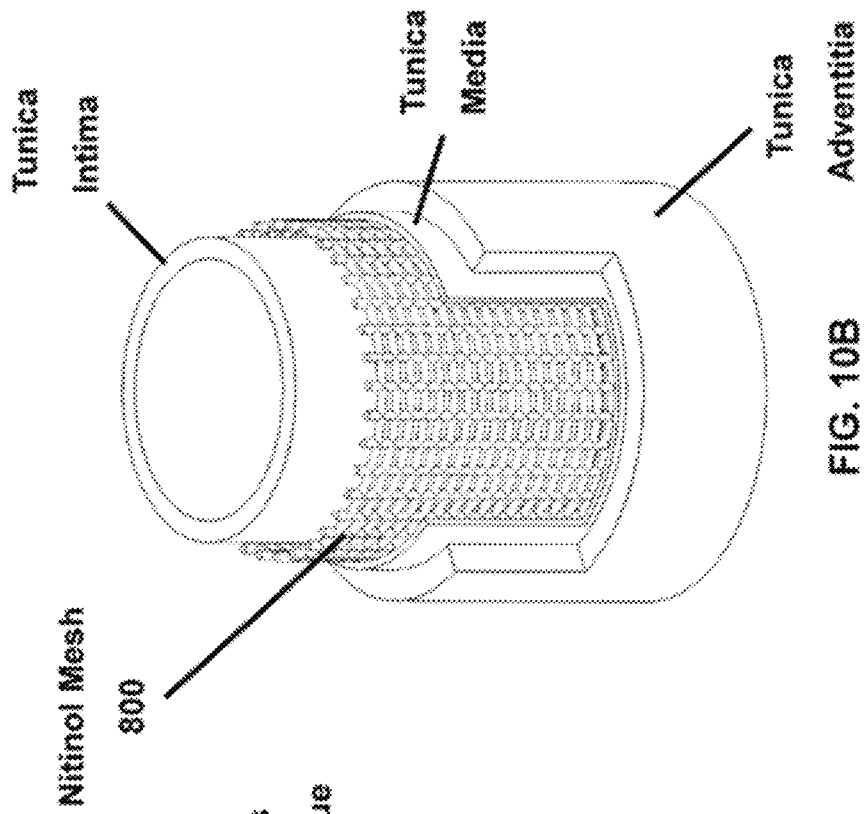


FIG. 10B

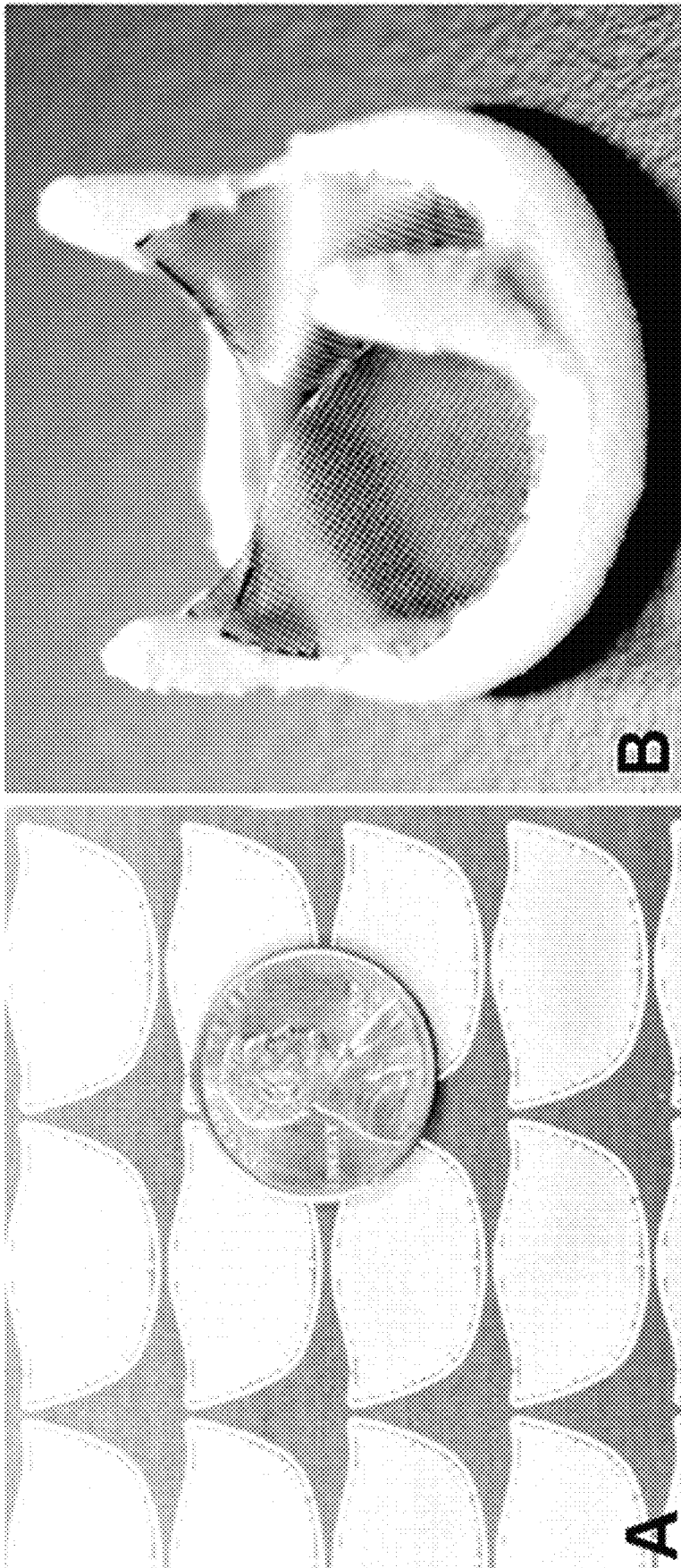


Fig. 11

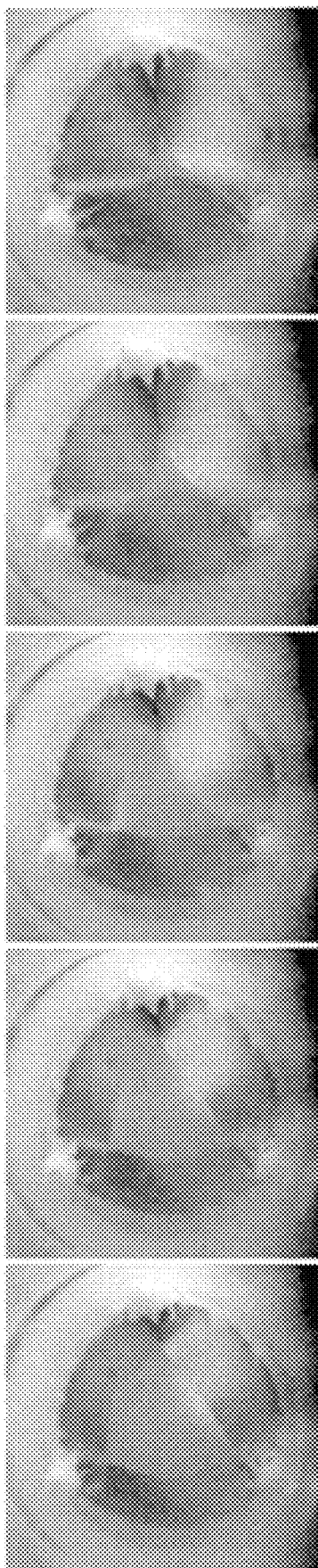


Fig. 12

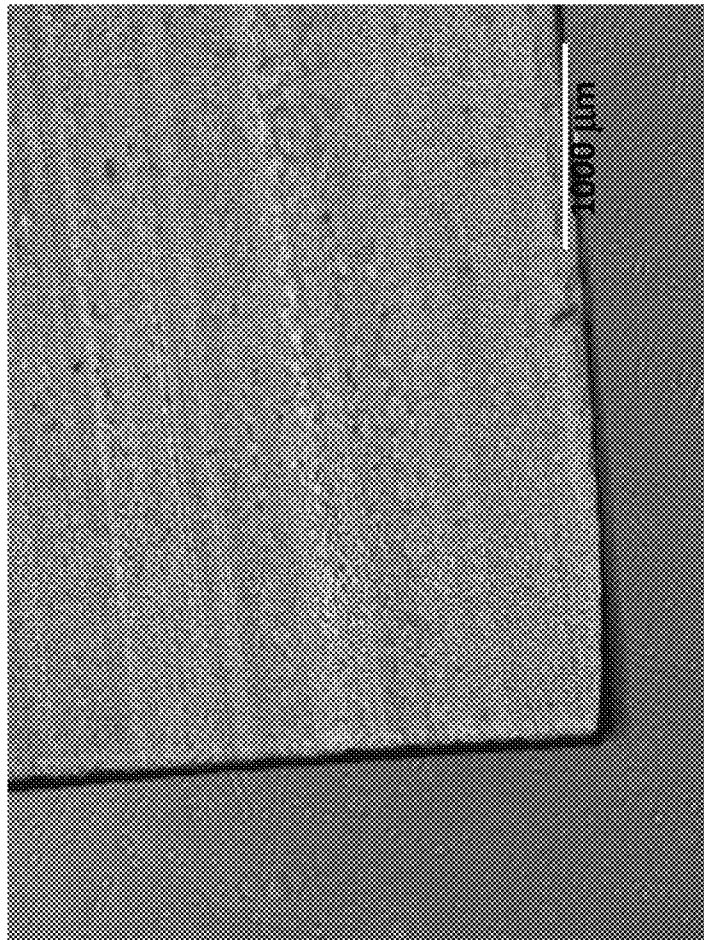


Fig. 13

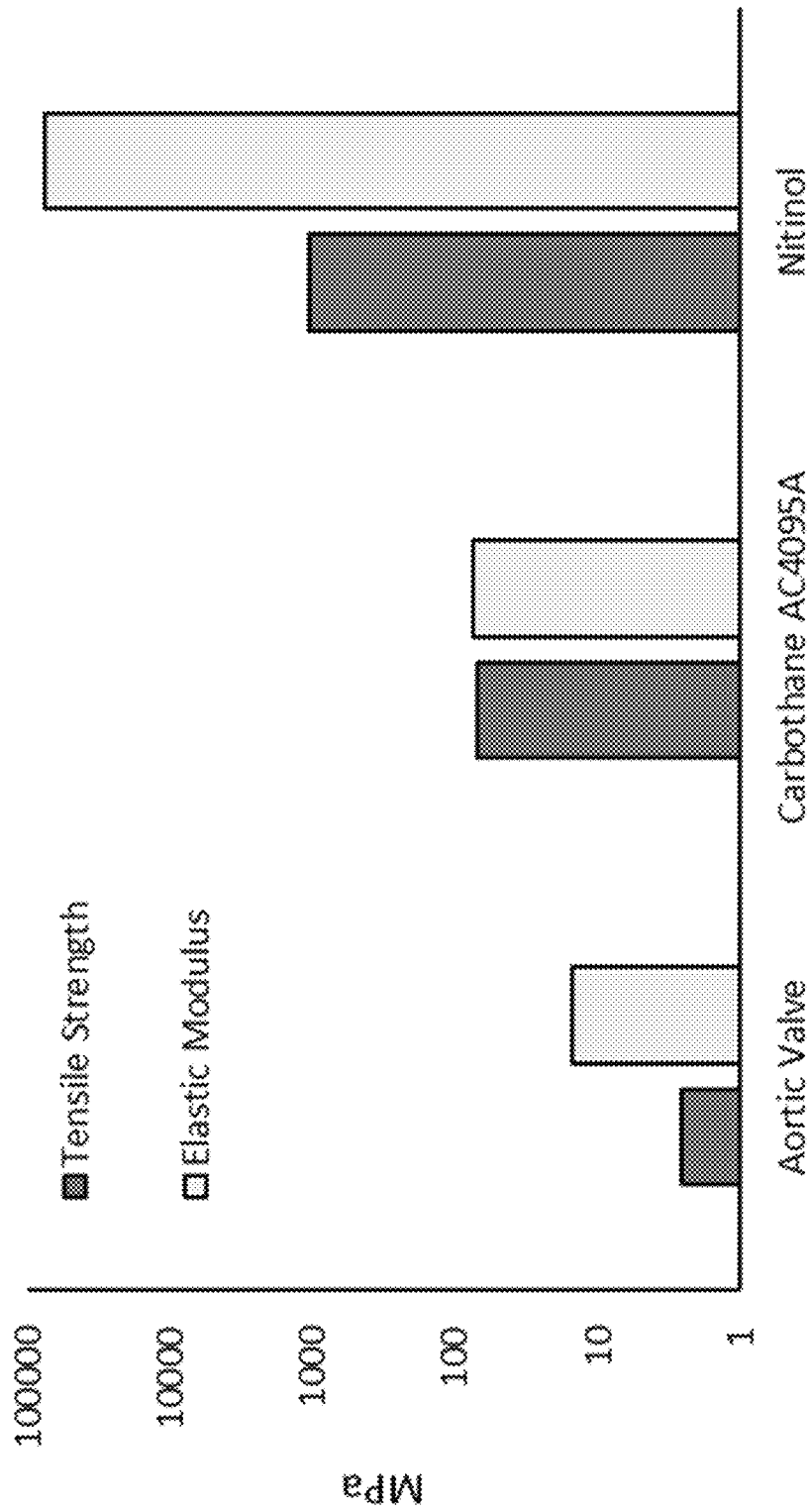


Fig. 14

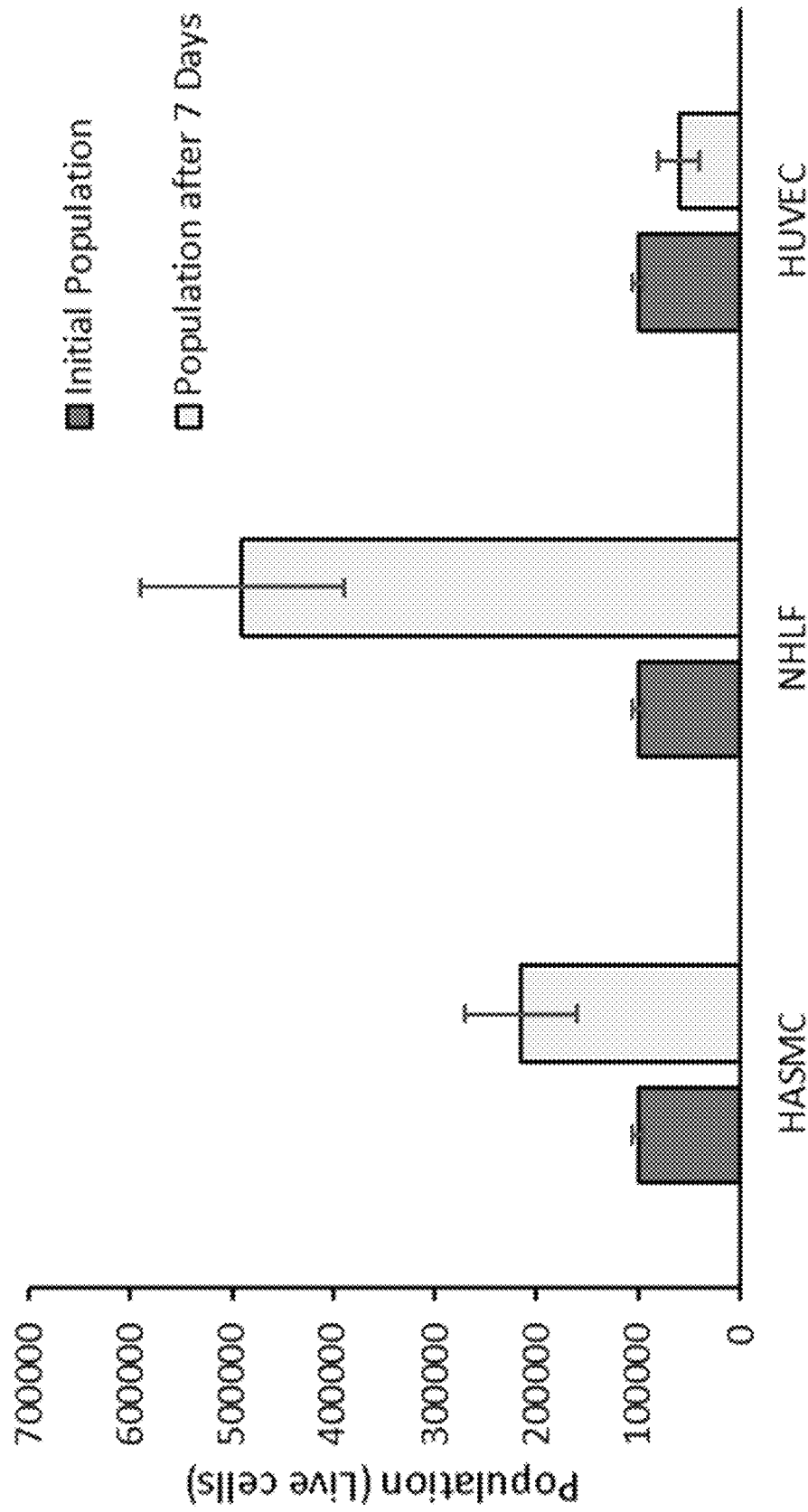


Fig. 15

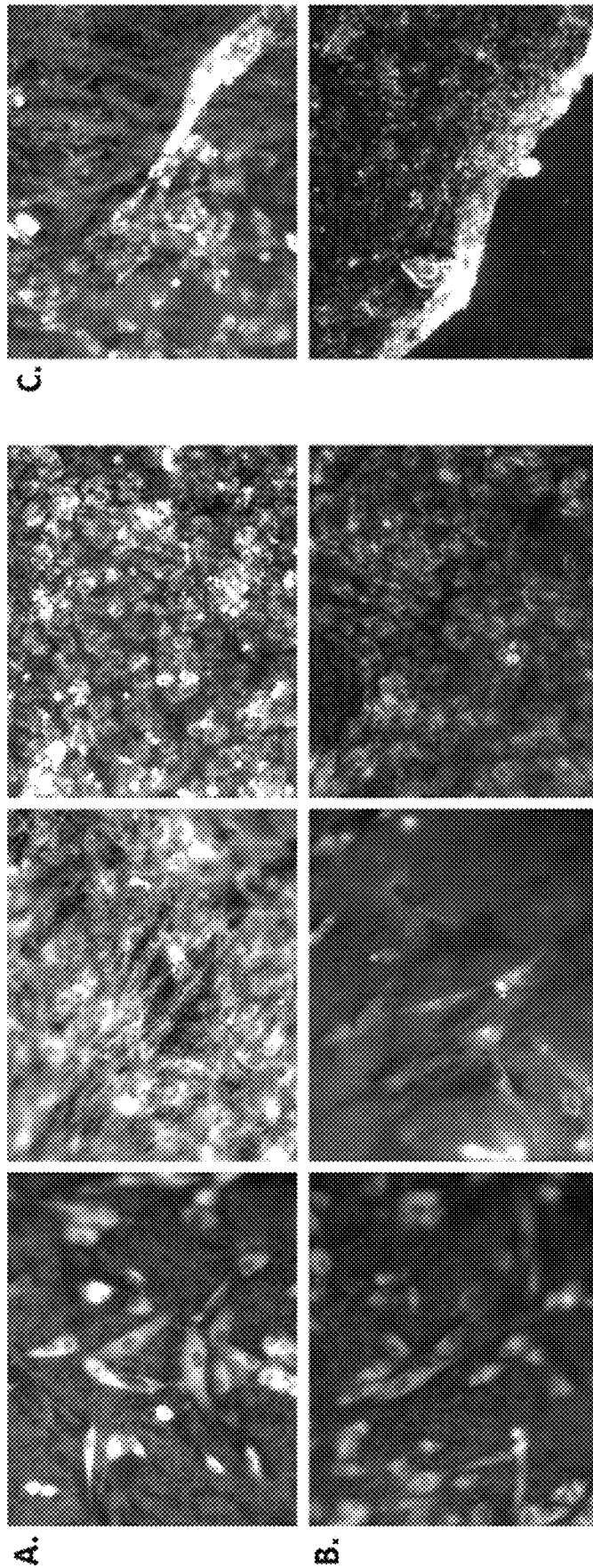


Fig. 16

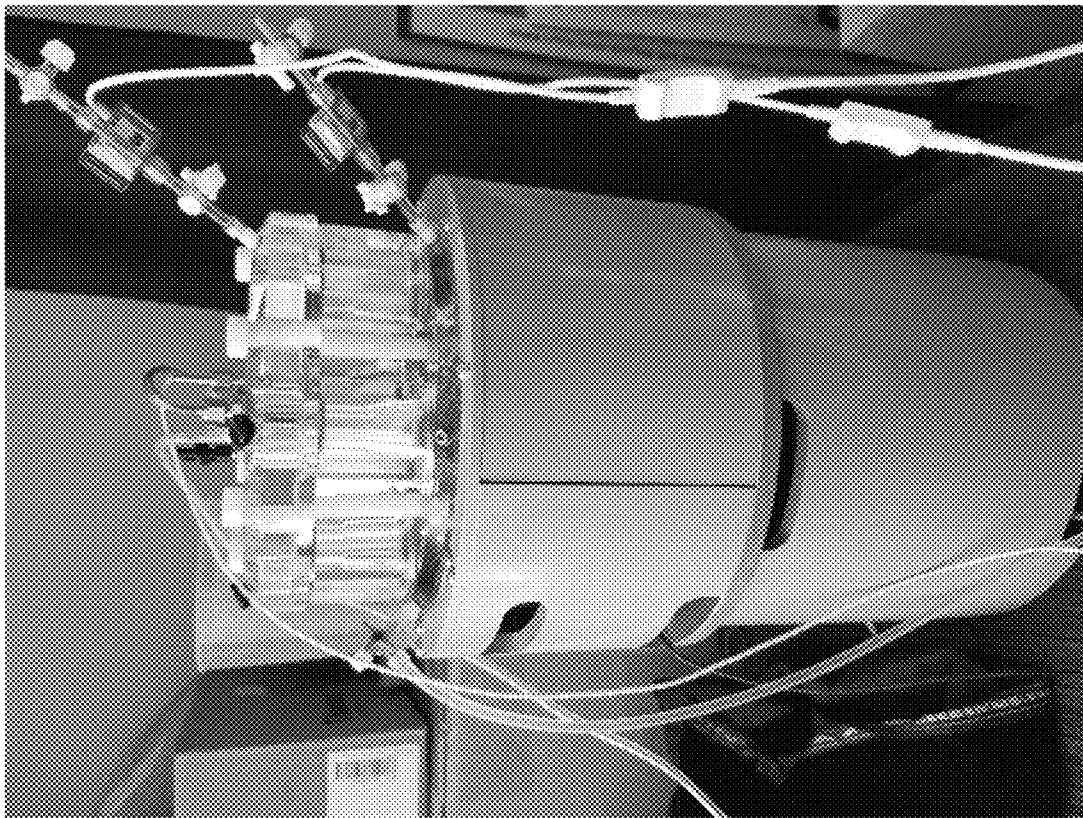


Fig. 17

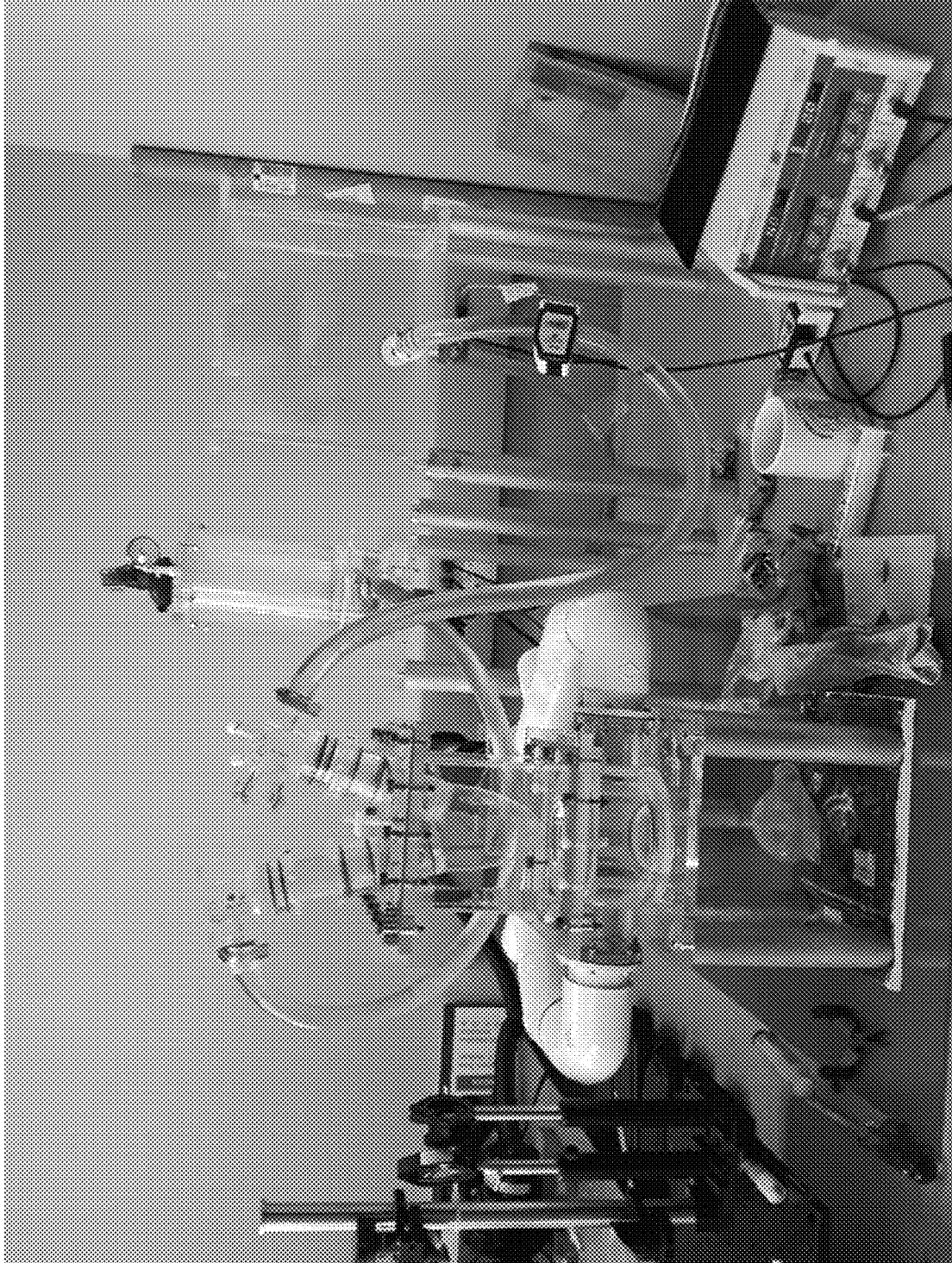


Fig. 18

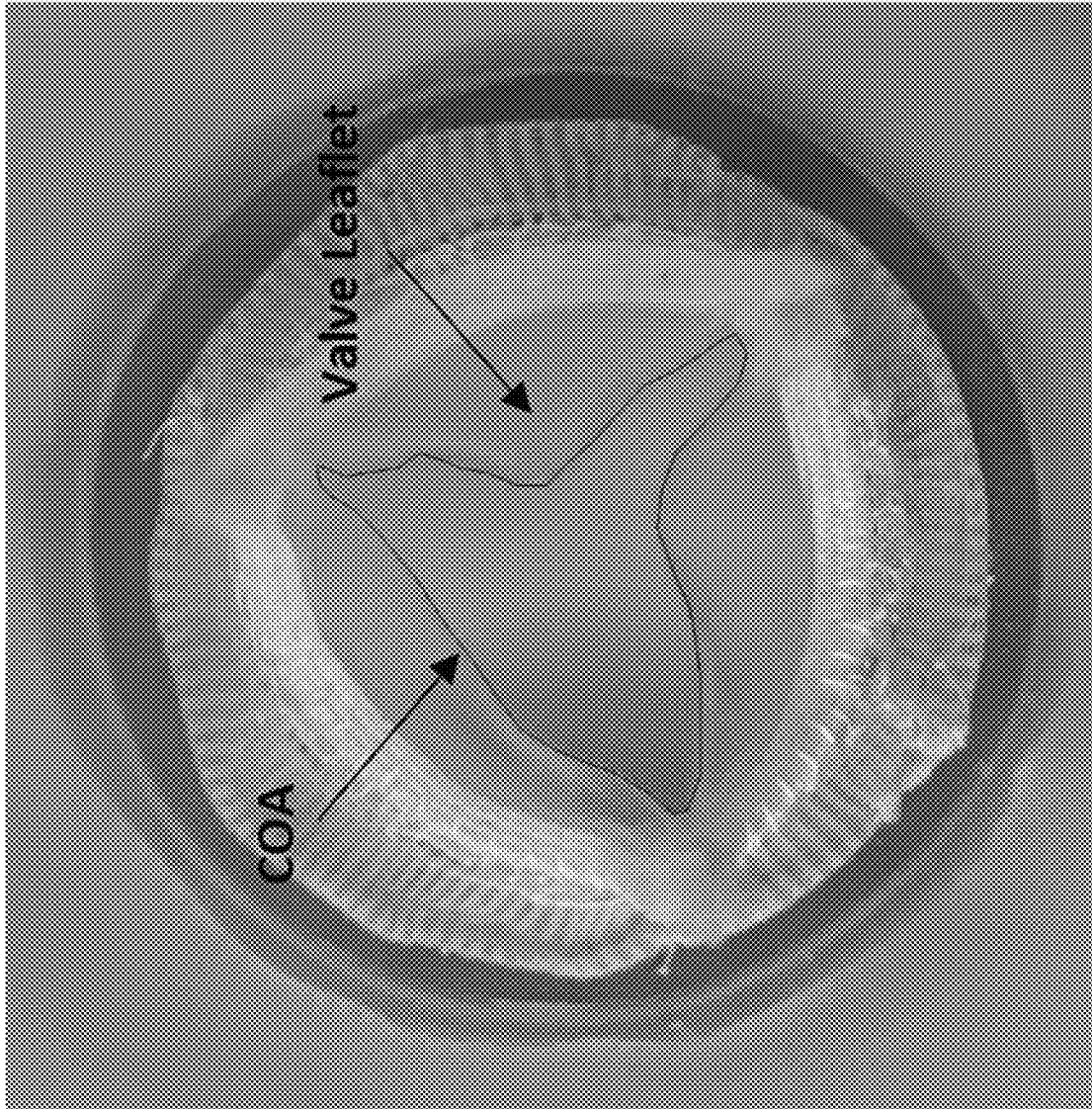


Fig. 19

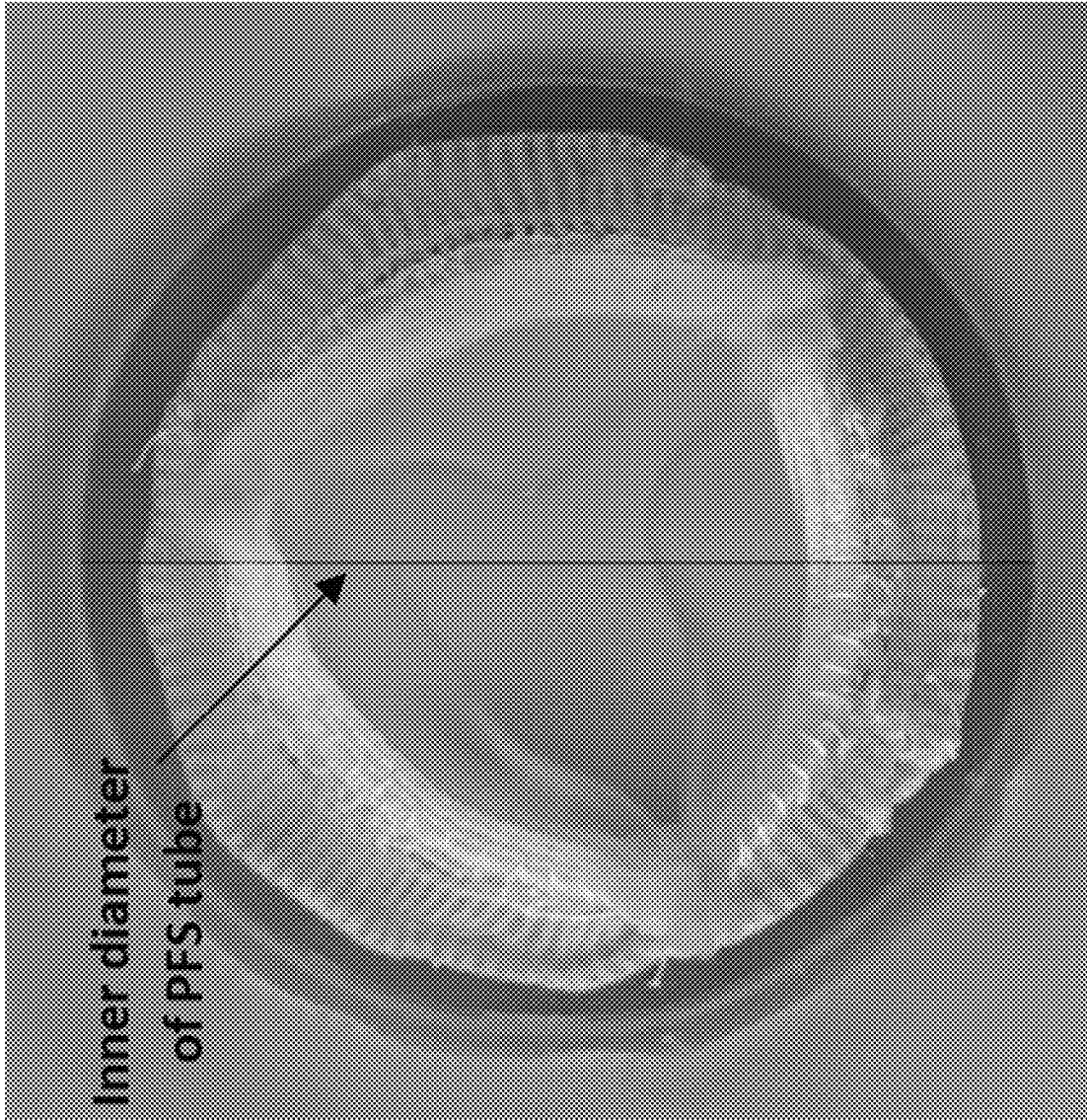


Fig. 20

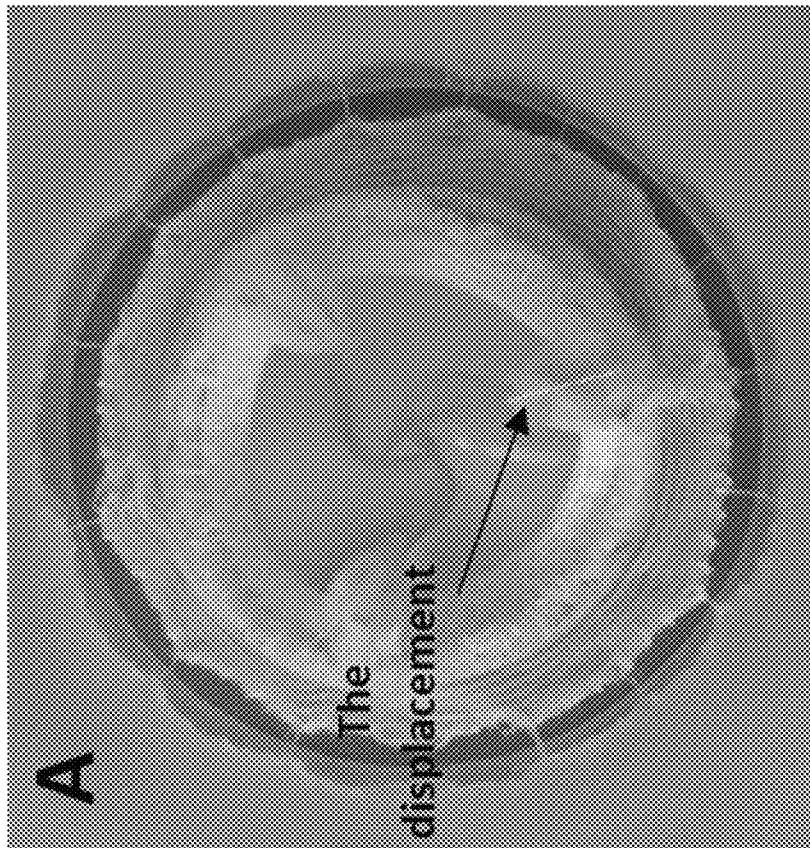
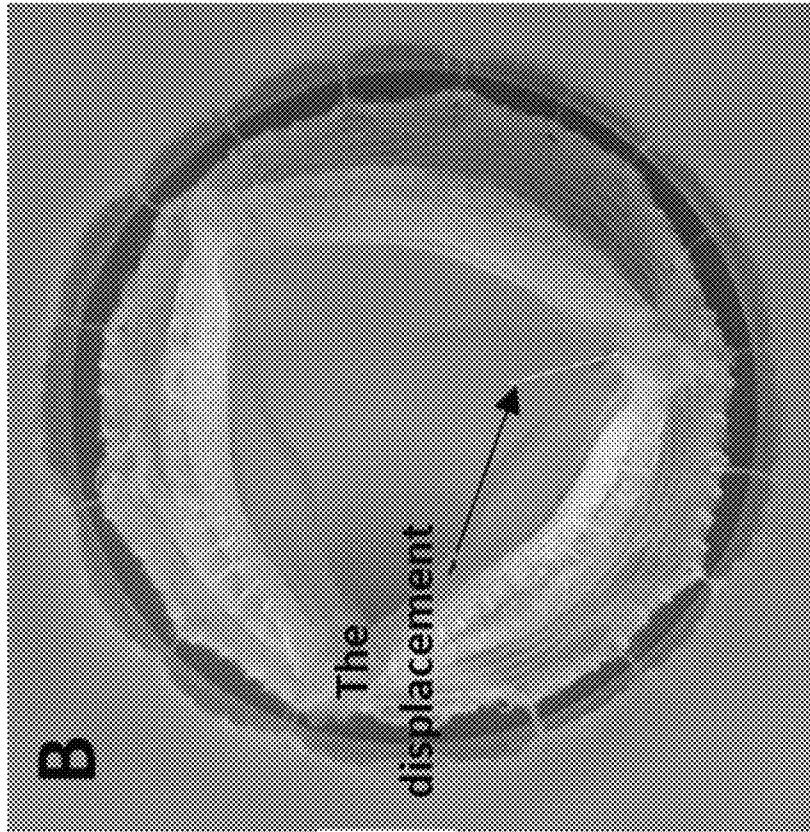


Fig. 21

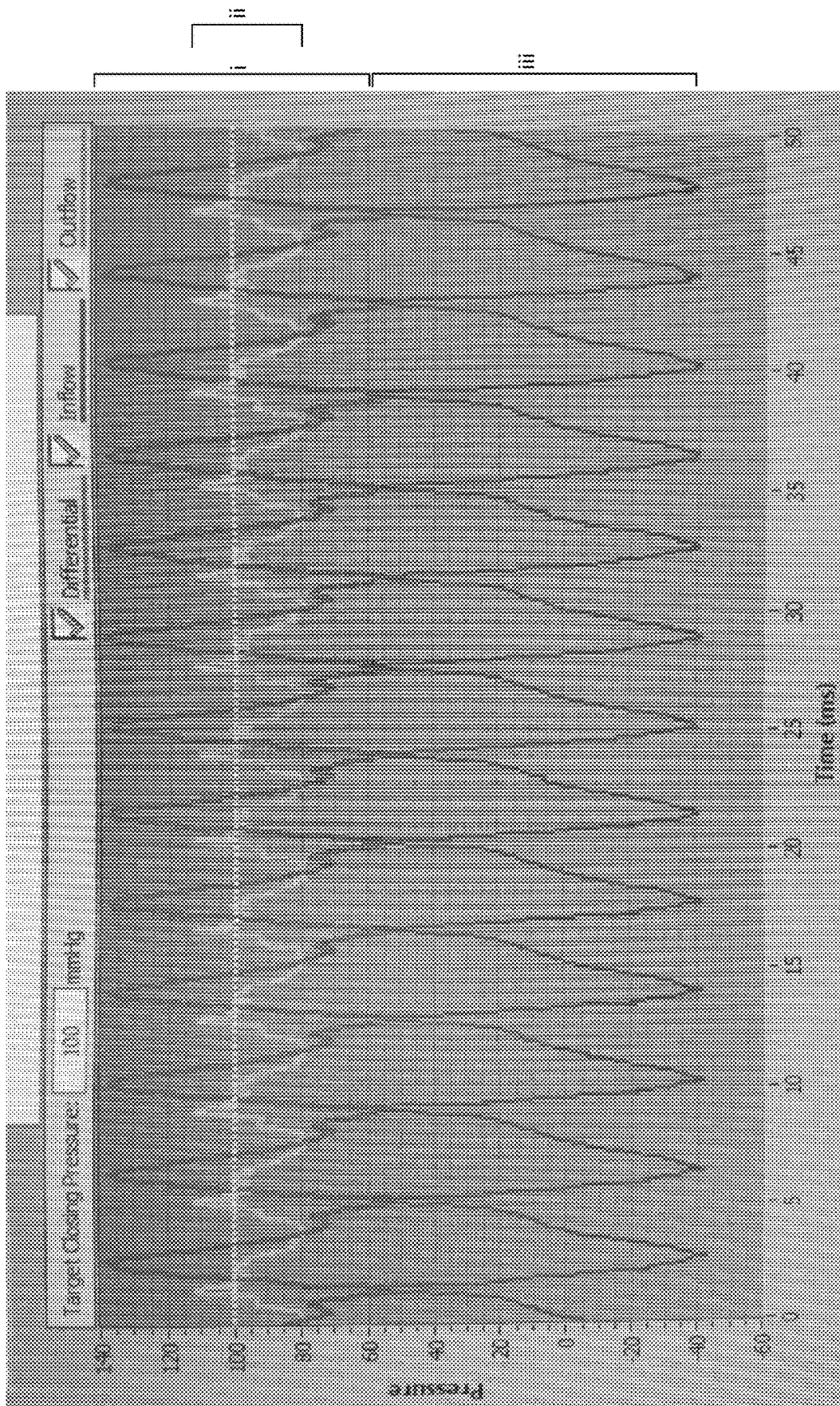


Fig. 22

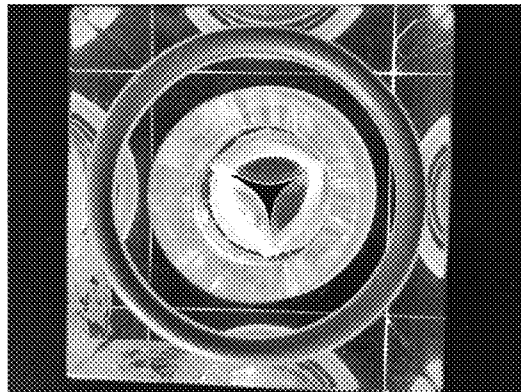
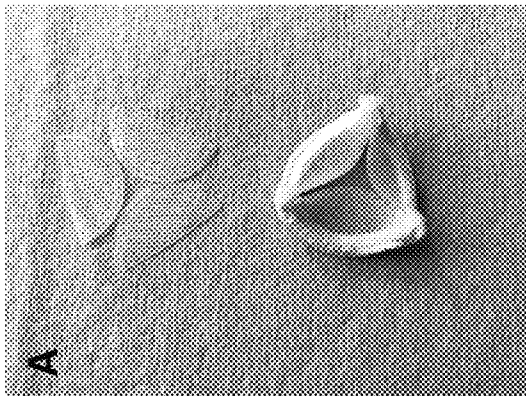
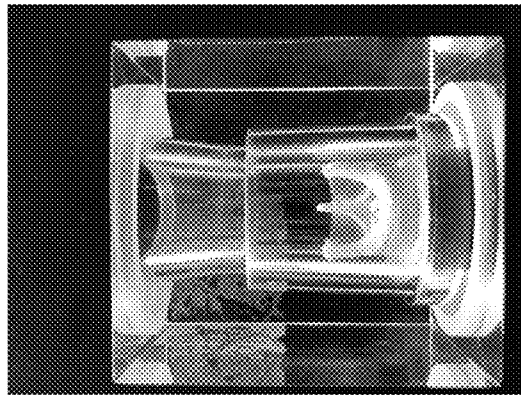
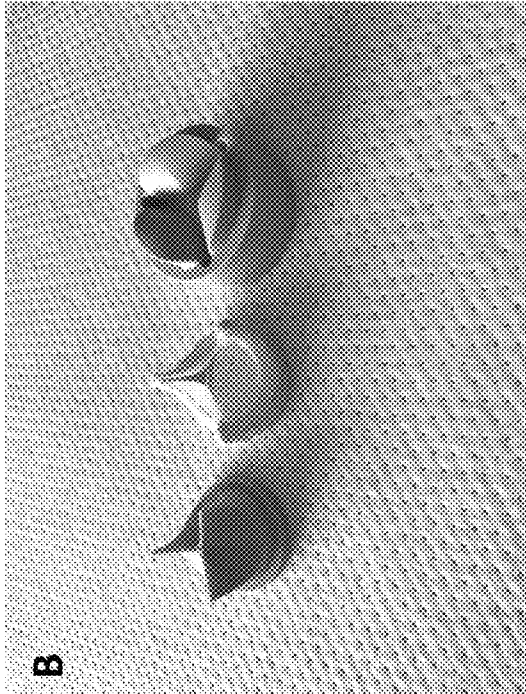


Fig. 23

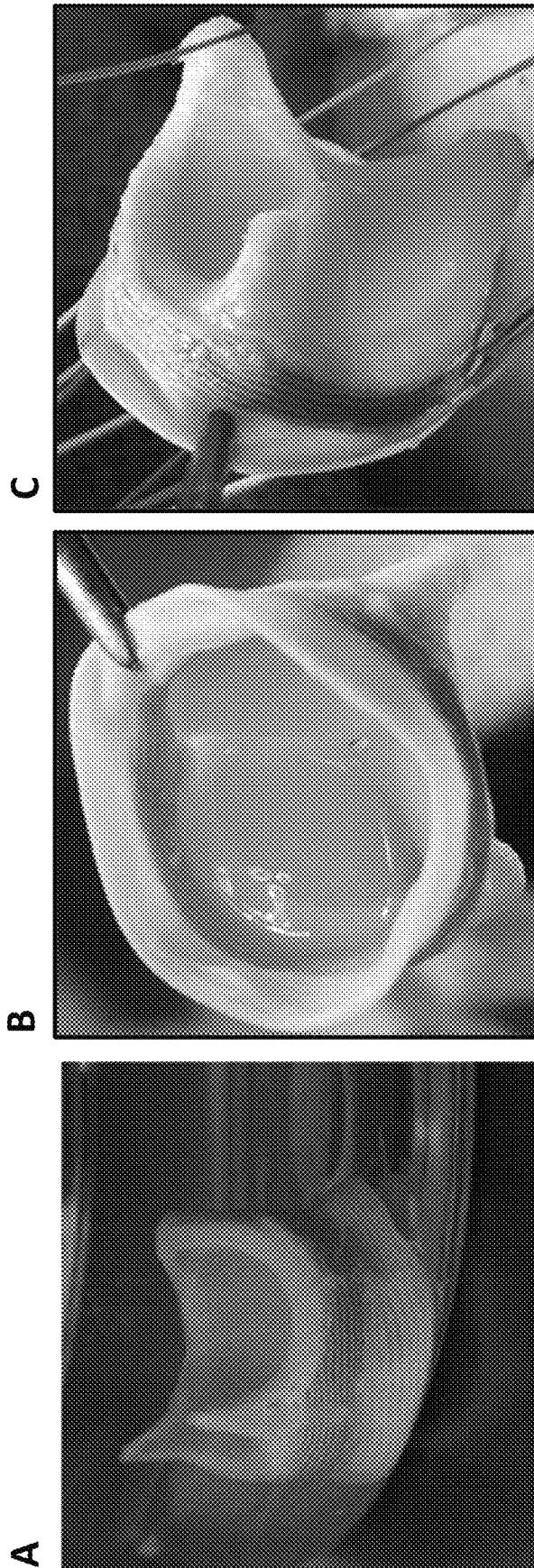


Fig. 24



Fig. 25

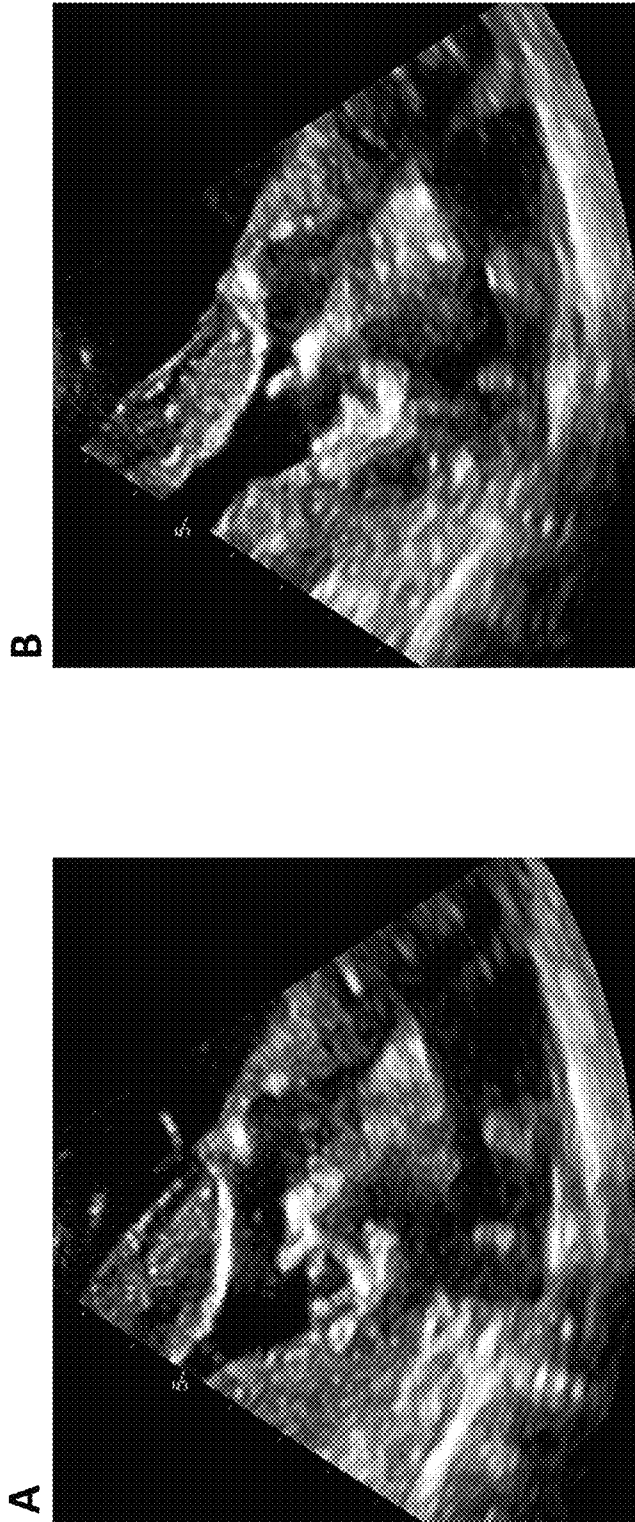


Fig. 26

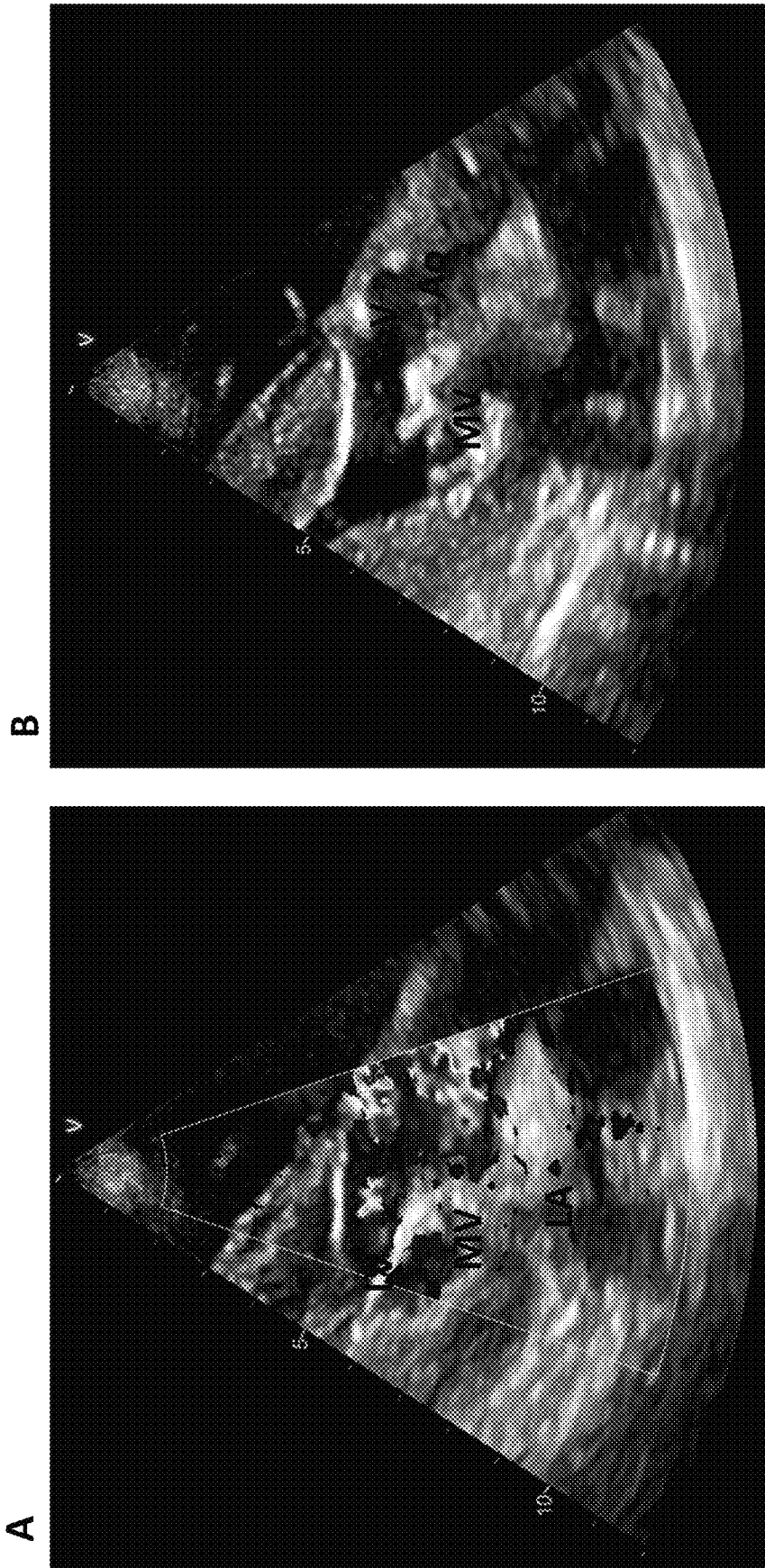


Fig. 27



Fig. 28

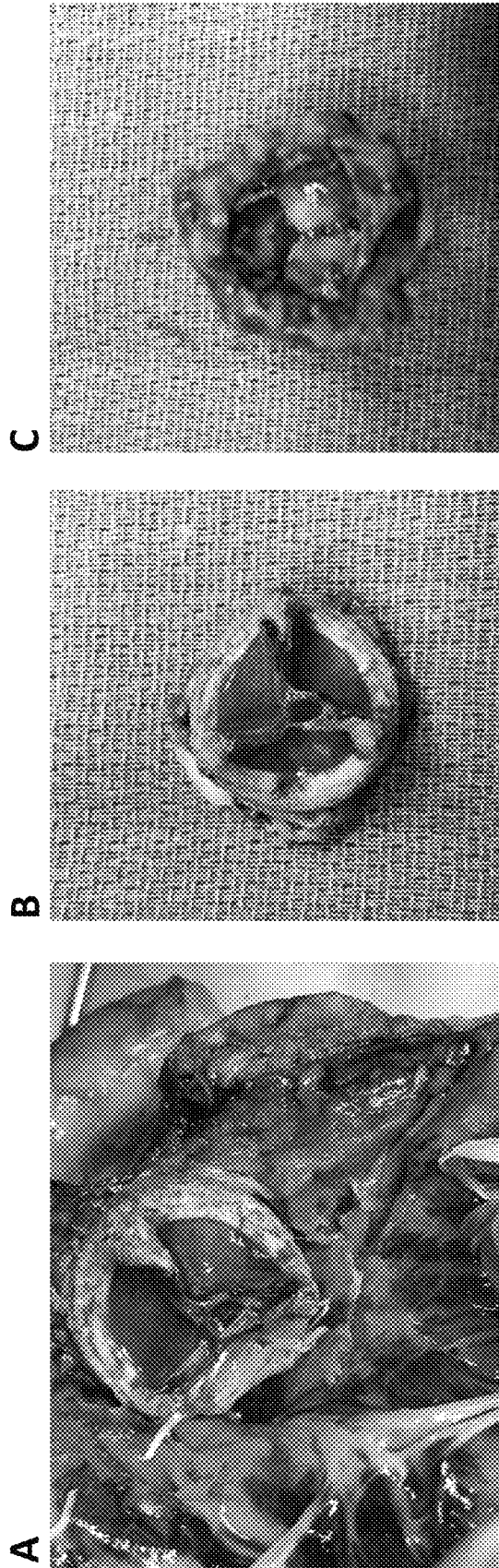


Fig. 29

MESH ENCLOSED TISSUE CONSTRUCTS

RELATED APPLICATIONS

This application is a continuation-in-part application of application Ser. No. 14/162,617, filed Jan. 23, 2014, which: (a) is a continuation-in-part application of application Ser. No. 13/427,807, filed Mar. 22, 2012, and (b) which claims priority to U.S. Provisional Application No. 61/756,451, filed Jan. 24, 2013; application Ser. No. 13/427,807 claims priority to: U.S. Provisional Application No. 61/559,694, filed Jan. 19, 2012, U.S. Provisional Application No. 61/540,330, filed Sep. 28, 2011, U.S. Provisional Application No. 61/496,369, filed Jun. 13, 2011, and U.S. Provisional Application No. 61/466,882, filed Mar. 23, 2011; all of which are herein incorporated by reference in their entireties.

FIELD

The disclosure pertains to a heart valve leaflet manufactured from a mesh material. The mesh material may have an ability to capture circulatory/stationary/migratory cells of the body to become biologically active.

BACKGROUND

Engineering of the membrane-like tissue structures with ability to remodel and regenerate is currently an unresolved subject in the field of tissue engineering. Several attempts with minimal success have been made to create functional viable membrane tissues such as heart valve leaflet with the ability to grow, repair, and remodel. Shinoka et al. fabricated single leaflet heart valves by sequentially seeding ovine fibroblasts and endothelial cells on a bioabsorbable polymer composed of a polyglactin woven mesh surrounded by two nonwoven polyglycolic acid mesh sheets. (See Shinoka, T., Breuer, C. K., Tanel, R. E., Zund, G., Miura, T., Ma, P. X., Langer, R., Vacanti, J. P., and Mayer J. E. Tissue engineering heart valves: Valve leaflet replacement study in a lamb model. *Ann Thorac Surg*, 60, 13, 1995). Hoerstrup et al. fabricated a trileaflet heart valve using nonwoven polyglycolic acid mesh, a bioabsorbable polymer, sequentially seeded with ovine myofibroblasts and endothelial cells made using a pulse duplicator in vitro system. (See Hoerstrup, S. P., Sodian, R., Daebritz, S., Wang, J., Bacha, E. A., Martin, D. P., Moran, A. M., Guleserian, K. J., Sperling, J. S., Kaushal, S., Vacanti, J. P., Schoen, F. J., and Mayer, J. E. Jr. Functional living trileaflet heart valves grown in vitro. *Circulation*, 102, 44, 2000). Sodian et al. constructed trileaflet heart valve scaffolds fabricated from seeding ovine arterial vascular cells on a polyhydroxyoctanoate material. (See Sodian, R., Hoerstrup, S. P., Sperling, J. S., Daebritz, S., Martin, D. P., Moran, A. M., Kim, B. S., Schoen, F. J., Vacanti, J. P., and Mayer, J. E. Jr. Early in vivo experience with tissue-engineered trileaflet heart valves. *Circulation*, 102, suppl III, 2000). Sutherland et al. created autologous semilunar heart valves in vitro using mesenchymal stem cells and a biodegradable scaffold made of polyglycolic acid and poly-L-lactic acid. (See Sutherland, F. W., Perry, T. E., Yu, Y., Sherwood, M. C., Rabkin, E., Masuda, Y., Garcia, A., McLellan, D. L., Engelmayr, G. C., Sacks, M. S., Schoen, F. J., and Mayer J. E. Jr. From stem cells to viable autologous semilunar heart valve. *Circulation*, 111, 2783, 2005). Drawbacks to the approaches described above include structural vulnerability, short term functionality, and limited mechanical properties of the membrane constructs.

Scaffolds are critical components of the engineered tissues that allow them to be formed in vitro and remain secure in vivo when implanted in a host. Several approaches have been taken to develop scaffolds for tissue membranes. The most widely used method involves biodegradable naturally-derived or synthetic polymers, where the polymer eventually degrades by normal metabolic activity, while the biological matrix is formed. To have viable tissue, the rate of scaffold degradation should be proportional to the rate of tissue formation to guarantee mechanical stability over time. The poor control of enzymatic degradation and low mechanical performance are two major limitations of naturally derived polymers. In contrast, synthetic polymers can be prepared precisely with respect to structure and function. However, most of them produce toxic chemicals when they degrade in vivo, and due to lack of receptor-binding ligands, they may not provide a good environment for adhesion and proliferation of cells.

Another option for creating scaffolds is to use decellularized xenogenic tissues, which has some advantages over polymeric materials. Decellularized tissues provide a unique scaffold, which is essentially composed of extracellular matrix (ECM) proteins that serve as an intrinsic template for cells. However, the process of decellularization cannot completely remove the trace of cells and their debris. These remnants not only increase the potential of an immunogenic reaction, but also result in increased tissue susceptibility to calcification.

Another, albeit less developed, strategy involves creating a scaffold with completely biological matrix components. This approach has advantages over using polymeric materials or decellularized xenogenic tissues. For example, large amounts can be produced from xenogenic sources, which can readily accommodate cellular ingrowth without cytotoxic degradation products. However, this strategy is restricted due to mechanical fragility of the scaffold and the low potentials for creating complex tissue structures.

Thus, a continuing need exists for a tissue construct that is strong enough to resist forces that exist inside a body, while possessing biocompatible surfaces.

SUMMARY

Some embodiments relate to a heart valve leaflet including a thermoplastic polyurethane (TPU) mesh material.

In some embodiments, the heart valve leaflet includes one to three layers of cells cultured on each side of the mesh material.

In some embodiments, the one to three layers of cells include smooth muscle cells, fibroblasts, and/or endothelial cell populations.

In some embodiments, the smooth muscle cells are vascular smooth muscle cells (VSMC).

In some embodiments, the one to three layers of cells cultured on each side of the mesh material include a first layer of smooth muscle cells formed directly on the thermoplastic polyurethane mesh, a second layer of fibroblast/myofibroblast cells formed on the first layer, and a third layer of endothelial cells formed on the second layer.

In some embodiments, a first layer of smooth muscle cells and fibroblast/myofibroblast cells are intermixed together and are formed directly on the thermoplastic polyurethane mesh, and a second layer of endothelial cells is formed on the first layer.

In some embodiments, the TPU mesh material includes an aliphatic polycarbonate-based thermoplastic polyurethane or an aromatic polycarbonate-based thermoplastic polyurethane.

In some embodiments, the thermoplastic polyurethane (TPU) mesh material has a tensile strength of about 68.9 MPa, an elastic modulus of about 74.5 MPa.

In some embodiments, the leaflet has an ability to capture circulatory/stationary/migratory cells of the body to become biologically active.

In some embodiments, the leaflet has a modified surface, which facilitates growth of a tissue layer on the leaflet, such that the mesh may become enclosed in the tissue layer.

In some embodiments, a bioactive material is used to coat the leaflet to optimize cell capture and/or to actively recruit cells and/or provide cell differentiation guidance.

In some embodiments, the bioactive material is selected from the group consisting of a molecule that binds to a cell adhesion molecule (CAM), a growth factor, an extracellular matrix molecule, a subendothelial extracellular matrix molecule and a peptide.

In some embodiments, the molecule that binds to a CAM is a CD34 antibody.

In some embodiments, the growth factor is selected from the group consisting of epidermal growth factor (EGF), fibroblast growth factor 1 (FGF1), FGF2, FGF3, FGF4, vascular endothelial growth factor-A (VEGF-A), VEGF-B, VEGF-C, VEGF-D, and placental growth factor (PGF).

In some embodiments, the subendothelial extracellular matrix molecule is selected from the group consisting of fibronectin, fibulin-5 and fibrillin-1.

In some embodiments, the peptide is an RGD-peptide.

In some embodiments, the surface of the leaflet is modified by plasma coating.

In some embodiments, the surface of the mesh is micro-patterned to enhance cell binding.

In some embodiments, the mesh has a stiffness that is comparable to a native heart valve leaflet, such that it functionally mimics a native heart valve leaflet.

In some embodiments, the mesh has a hole diameter of between 0.0005-0.0400 inches.

In some embodiments, the mesh has no physical holes.

In some embodiments, the mesh has a hole diameter of about 0.0088 inches.

In some embodiments, the mesh has a thickness of between 0.0004-0.0100 inches.

In some embodiments, the mesh has a thickness of about 0.001 inches.

Some embodiments relate to a heart valve including a heart valve leaflet as disclosed herein.

In some embodiments, the heart valve includes a metal frame.

In some embodiments, the metal frame includes titanium.

In some embodiments, the metal frame is 3D printed.

In some embodiments of heart valve, the thermoplastic polyurethane (TPU) mesh material has a tensile strength and an elastic modulus that are within an order of magnitude from the tensile strength and elastic modulus of native aortic valve tissue, and wherein the heart valve withstands 50 million cycles with no detectable damage on the frame and leaflets.

In some embodiments, the thermoplastic polyurethane (TPU) mesh material has a tensile strength of about 68.9 MPa, an elastic modulus of about 74.5 MPa.

BRIEF DESCRIPTION OF THE DRAWINGS

The objects, features and advantages of the present invention will be apparent from the following detailed descrip-

tions of the preferred aspect of the invention in conjunction with reference to the following drawings where:

FIG. 1A shows a representation of a scaffold of one aspect of the present invention;

FIG. 1B is a diagram showing the three layers of cells of a scaffold that mimic heart valve tissue structure of one aspect of the present invention;

FIG. 2 is a schematic showing the steps in the three-dimensional (3D) cell culture method to develop a tissue;

FIG. 3A is an image of a stainless steel mesh with a surface area of about 1 cm.^{sup.2};

FIG. 3B is a view of the engineered tissue after three months of cell culture;

FIG. 4A is a scanning electron micrograph of the first layer on the mesh showing that smooth muscle cells are attached over the mesh;

FIG. 4B is an expanded view of FIG. 4A;

FIG. 5A is a scanning electron microscopy image taken after culturing the second layer of cells containing fibroblasts and myofibroblasts;

FIG. 5B shows the formation of extracellular matrix and a layer of cells formed on the metal mesh, the black arrow indicates a single fibroblast cell;

FIG. 6A shows a top view of cell culture without addition of TGF- β ;

FIG. 6B shows a top view of cell culture without addition of TGF- β ;

FIG. 6C shows the top view of the cell culture with TGF- β added to the cell culture;

FIG. 6D shows the top view of the cell culture with TGF- β added to the cell culture;

FIG. 7A is a scanning electron microscopy image that show layers of tissue tightly enclosing the stainless steel mesh;

FIG. 7B is a scanning electron microscopy image that show three layers of tissue tightly enclosing the stainless steel mesh;

FIG. 7C is a scanning electron microscopy image that show three layers of tissue tightly enclosing the stainless steel mesh;

FIG. 7D is a scanning electron microscopy image that show three layers of tissue tightly enclosing the stainless steel mesh;

FIG. 8A is an illustration depicting a size comparison of a one-centimeter by one-centimeter Nitinol mesh in relation to a United States Penny;

FIG. 8B shows the engineered tissue on Nitinol mesh after the months of cell culture;

FIG. 9A is an illustration of a heart valve depicting the Nitinol mesh scaffolding;

FIG. 9B is an illustration of a heart valve with heart leaflets that are made of tissue described in this application;

FIG. 9C is an illustration of a heart valve with heart leaflets that are made of tissue described in this application;

FIG. 9D is an illustration depicting schematic parts of a tri-leaflet scaffold that can be used as a heart valve;

FIG. 9E is an illustration that includes various view-point illustrations of the heart valve;

FIG. 9F is an image of the tri-leaflet scaffold that is depicted in FIGS. 9A and 9D;

FIG. 10A is a schematic representation of a blood vessel; and

FIG. 10B is a schematic representation of a blood vessel formed from the tissue described in this application.

FIG. 11 depicts a Nitinol mesh leaflet and the bioactive valve. (A) The flat Nitinol mesh cut to the desired shape of a leaflet; (B) a tri-leaflet valve comprised of a stand, a base

and leaflets made of 25 microns thickness Nitinol mesh leaflets. The surface of the mesh has been modified to become biologically active once implanted to capture the cells of the body.

FIG. 12 depicts functional testing of a tri-leaflet bioactive valve with Nitinol mesh leaflets inside a heart flow simulator. The images are consecutive slides taken from a recorded movie showing opening and closure of the valve. It can be seen that the leaflets are compliant enough to open and close with a flow rate (3 L/min) even less than normal flow rate of the heart.

FIG. 13 shows a thermoplastic polyurethane (TPU) scaffold material. A thin film sheet of CARBOTHANE was used in biocompatibility tests. 1 cm² pieces were cut and placed in individual culture wells.

FIG. 14. Elastic modulus and tensile strengths of scaffold materials. The mechanical properties of aortic valves (left) compare more favorably with those of CARBOTHANE (middle) than Nitinol (right).

FIG. 15. HASMC, NHLF, and HUVEC cell populations. Only HUVEC populations decreased over the duration of the experiment.

FIG. 16. Fluorescence microscopy images of HASMCs, NHLFs, and HUVECs on AC-4095A. (A) HASMCs (left), NHLFs (middle), and HUVECs (right) show attachment on fibronectin-treated AC-4095A. (B) Attachment is seen for cells on untreated AC-4095A. (C) HUVECs begin to clump together and die on fibronectin-treated (top) and untreated (bottom) AC-4095A within 24 hours.

FIG. 17. Accelerated Wear Testing (AWT) M6 simulator with pressure sensors.

FIG. 18. Pulsatile Flow Simulator (PFS) with associated equipment.

FIG. 19. Valve in the opened position and measurement of circulated orifice area (COA) (Valve 1 at 3.6 L/min).

FIG. 20. Valve in the opened position and method of image calibration. (Valve 1 at 3.6 L/min).

FIG. 21. Post displacement calculated from the valve at the closed (A) and opened (B) positions. The white line shows the post displacement. (Valve 2 at 4.4 L/min).

FIG. 22: Inlet and outlet pressure measured by DYNATEK software. The traces marked (i), (ii) and (iii) represent the inflow, outflow and the differential pressure, respectively.

FIG. 23. Manufacture and testing of tri-leaflet valve. (A) Three CARBOTHANE mesh leaflets are sewn into a tri-leaflet valve. (B) CARBOTHANE mesh scaffold with culture male/female molds. (C) and (D) CARBOTHANE valve (not-meshed) in the Accelerated Wear Testing (AWT) M6 simulator ready for testing.

FIG. 24. A hybrid valve with a titanium frame and a polyurethane core. (A) In culture medium. Covered by collagen fibers and endothelial cells on both sides, (B) aortic side and (C) ventricular side.

FIG. 25. Surgical mitral valve replacement. Hybrid valve prior to implantation (A) and during attachment with sutures in the mitral position (B).

FIG. 26. Mobility of leaflets in hybrid valve during: (A) systole, the phase of the heartbeat when the heart muscle contracts and pumps blood from the chambers into the arteries and (B) diastole, the phase of the heartbeat when the heart muscle relaxes and allows the chambers to fill with blood.

FIG. 27. Regurgitation Analysis. No regurgitation was observed in the implanted valve at mitral position after surgery. (A) Doppler imaging shows that no blood regurgitates when the valve is closed during systole, (B) Structural

image shows the valve positioned and working at mitral position. Left ventricle, LV; mitral valve, MV; left atrium, LA; and aorta, Ao.

FIG. 28. Postoperative Status: Mitral valve replacement was successfully performed and the sheep was able to walk around and drink water after recovery from anesthesia.

FIG. 29. Post-implantation analysis of hybrid valve following surgical removal approximately six hours after the implantation. (A) Hybrid valve in the mitral position. Removed hybrid valve was covered by intact collagen fibers and endothelial cells on the (B) ventricular and (C) aortic sides. The images show that the hybrid valve is intact with all tissues still in place, neither washed nor detached from the CARBOTHANE scaffold.

DETAILED DESCRIPTION

Reference will now be made in detail to embodiments of the present disclosure, examples of which are illustrated in the accompanying drawings. While the disclosure will be described in conjunction with these embodiments, it will be understood that they are not intended to limit the invention to these embodiments. On the contrary, the disclosure is intended to cover alternatives, modifications, and equivalents, which may be included with the spirit and scope of the invention as defined by the appended claims. Furthermore, in the following detailed description, numerous specific details are set forth in order to provide thorough understanding of the present disclosure. However, it will be recognized by one of ordinary skill in the art that the present disclosure may be practiced without these specific details. In other instances, well-known methods, procedures, and components have not been described in detail as not to unnecessarily obscure aspects of the embodiments.

As noted above and as shown in FIG. 1A, some embodiments are directed to a scaffold **100** that is composed of multi-layered tissue enclosed on a metal mesh. This is further illustrated in FIG. 1B, which illustrates that the scaffold **100** is made of an extra layer of metal mesh **102** enclosed by a biological matrix, such as layers (e.g., three layers) of cells (e.g., different cell types). It should be understood that while embodiments of the present disclosure are described as scaffold **100** that includes three layers of different cell types, it is not intended to be limited thereto as the scaffold **100** can be formed with a single layer, or any suitable number of layers, and, further, with a single or different cell types. Additionally, while the mesh **102** is described as being covered with biological materials or a biological matrix, the disclosure is not limited thereto as the mesh **102** can also be enclosed by synthetic materials that are known to one skilled in the art (such as polymers, etc.). As a non-limiting example, the synthetic material can be molded onto the mesh. Such as

However, desirably, the three layers of biological materials include a first layer **104** of smooth muscle cells. The second layer **106** may be composed of fibroblast and myofibroblast cells and the third layer **108** (which can be the outer layer) may comprise of endothelial cells. These three layers wrap around the metal mesh **102** in three-dimensions so that each layer fully envelopes the metal mesh **102**. This approach is intended to retain all the advantages of using biological scaffolds while developing a strong extracellular matrix (ECM) backbone composed of the mesh **102** that can withstand various types of loads after implantation inside the body. Additionally, such a mesh pattern ensures structure integration of the formed tissue and allows cells and ECM components on both sides of the mesh **102** to interact with

each other. The formed tissue is intended to be biomechanically resilient against the physiological stresses inside the body. In one aspect, the scaffold **100** is a living tissue, able to continually remodel and mature in vitro and in vivo. For example, the scaffold **100** has living tissue (as described below) that can continue to grow and mature, with the mesh **102** becoming biologically active when implanted in-vivo.

In one aspect, the three layers of cells of the scaffold **100** may mimic the heart valve structure. These three layers mimic ventricularis, spongiosa and fibrosa layers of a heart valve leaflet. This type of scaffold can be used in any membrane tissue fabrication, such as heart valve leaflets, vascular grafts, etc.

While the present disclosure is directed to a unique hybrid scaffold **100** as shown in FIGS. **1A** and **1B**, the present disclosure also includes the method of making the novel scaffold (made of an extra layer of metal mesh enclosed by three layers of different cell types). For example, FIG. **2** shows a schematic diagram of a method for producing the multilayered tissue. Through the three-dimensional cell culture technique detailed in this application, all layers of the cells were seeded on rectangular-shaped Stainless Steel meshes to produce ECM or connective tissue.

The method of making the multilayered tissue is as follows. The first step in creating the scaffold is preparation of the metal mesh scaffold. The metal mesh is any suitable material that can operate as scaffolding for a tissue. As a non-limiting example, the metal mesh may be a flat mesh of T316 Stainless Steel woven from 0.0037" round wires, targeting at 80 end per inch (EPI)×80 pick per inch (PPI) that possesses an opening size of 0.0088". A non-limiting example of such a mesh is that sold by TWP, Inc., located at 2831 Tenth Street, Berkeley, Calif. 94710 USA. The metal mesh was heated at 520° C. for 5 min, followed by water quenching. The oxidized film was removed at multiple stages; by polishing the surface, using hydrochloric acid wash, ultrasonic cleaning wash in ethanol for 15 min and glow discharging for 40 seconds. Finally, the mesh was cut into pieces with area of one square centimeter to be used for cell culture.

After the metal was cleaned and cut into pieces, an ion beam surface modification method was used to get a smooth surface and ensure the biocompatibility and enhanced cell attachment for the Stainless Steel meshes. The meshes were mechanically polished with wetted metallographic polishing high-grade Silicon Carbide (SiC) papers. Afterward, the meshes were acid-washed, degreased in an ultrasonic vibrobath, and rinsed with distilled water. Prior to cell culture, the samples were irradiated by He⁺ ion beam at energy of 150 keV with fluences of 1×10¹⁴ ions/cm².

In one aspect, the growth of the tissue may be aided by the addition of growth factors and materials. For example, a mixture containing bovine and rat tail collagen may be used to coat the mesh to ensure development of an interconnected pore network, which is essential for cell growth, nutrient supply, and removal of metabolic waste products. In addition, the culture media may be supplemented with additives, including, but not limited to, ascorbic acid to promote matrix production. Moreover, proteins (cytokines), including TGF-β1, may be added to the collagen gels in each layer to increase the rate of extracellular matrix production. For the biological part of the scaffold any collagen type by itself or in mixture as well as the other biological scaffold such as fibrin or even synthetic scaffolds can be used. Growth factors depending on the target tissue and the cells that have been used can be different, such as vascular endothelial

growth factor (VEGF) if endothelial progenitor cells are used instead of endothelial cells.

After the mesh has been prepared, the three-dimensional tissue scaffold was constructed by sequential seeding of three different types of cells on the metal mesh. As a non-limiting example, three different cell types were isolated and used for preliminary assay, as follows: smooth muscle cells and fibroblast and myofibroblast cells to fulfill the role of valvular interstitial cells (VICs) and endothelial cells to act as the valvular endothelial cells. In another aspect, the following three different cell types are isolated and used: human aortic smooth muscle cells, human aortic adventitial fibroblast/myofibroblast cells to fulfill the role of valvular interstitial cells (VICs), and human umbilical vascular endothelial cells to act as valvular endothelial cells. The basal media for culturing cells contained DMEM (e.g., Dulbecco's Modified Eagle Medium, Gibco, produced by Invitrogen Corporation, located at 1600 Faraday Ave., Carlsbad, Calif. 92006, USA), 10% fetal bovine serum (HyClone, Rockford, Ill.), 1% penicillin/streptomycin (Gibco, Carlsbad, Calif.) and 1% L-glutamine (Gibco, Carlsbad, Calif.), with appropriate growth factors added to it for enhancement of growth and proliferation. Cultured cells were fed every two to three days, and split 1 to 3 at confluence. Cells were used on the passages 3 to 5 for the experiment.

Each mesh was coated with a mixture of bovine and rat tail collagen (Gibco, Carlsbad, Calif.) in a tissue culture hood with an aligned appearance. The liquid collagen mixture was neutralized using NaOH. Cell-seeded collagen constructs were prepared by first casting an acellular collagen solution and then adding a total of 3×10⁶ cells for each cell type to it, before the collagen had set. After placing the Stainless Steel meshes among the solutions, the constructs were incubated at 37° C. in a 5% CO₂ humidified incubator for polymerization. This method ensures that collagen constructs have uniform cell density (3×10⁶ cells/cm²) after gel formation. The tissue constructs were cultured at 37° C. with replacement of culture media every two days. To achieve a phenotype similar to the natural valve leaflets in-vivo, the cells in the next layers were plated over the constructs at time intervals of two weeks and the next layer was constructed around the deeper layer in a similar method that has been described in the beginning of this paragraph. The media was also supplemented with ascorbic acid (e.g., produced by Sigma-Aldrich Inc., located at 3050 Spruce Street, St. Louis, Mo. 63103, USA) as an additive to promote matrix production. To increase the rate of extracellular matrix production, 10 ng/ml of TGF-β1 (e.g., produced by R&D Systems Inc., located at 614 McKinley Place Northeast, Minneapolis, Minn. 55413, USA) was added to the collagen gels in each layer. These cultures were later on compared to the control group with no TGF-β supplementation.

In one aspect, the tissue may be suitable for applications in which strong composition of the membrane is essential, including but not limited to, heart valves and vascular grafts. For further understanding, FIGS. **3A** and **3B** provide images that depict the scale and size of the mesh and corresponding tissue. For example, FIG. **3A** is an image of a stainless steel mesh **102** with a surface area of about one square centimeter. Additionally, FIG. **3B** is a macroscopic view of the engineered tissue **100** after three months of cell culture. The outer surface shown in FIG. **3B** is the endothelial layer or the third layer. Seeding the third layer completely concealed the mesh **102** and formed a smooth, confluent surface around the construct. Although the third layer concealed the mesh **102**, the metallic mesh **102** can still be seen inside the tissue.

FIG. 4A and FIG. 4B are scanning electron micrographs (SEM) images of the first layer of cells. FIG. 4A shows the smooth muscle cells **400** as being attached over the mesh **102**. FIG. 4B shows the first layer of tissue (i.e., the smooth muscle cells **400**) compacted during the culture period, which confirmed the expression of alpha-SMA, as its expression.

FIG. 5A is a top-view of the SEM image taken after culturing the second layer of cells containing fibroblasts/myofibroblasts. Formation of ECM and a confluent layer around the construct are visible. Alternatively, FIG. 5B shows a side-view of the SEM image. The arrow in FIG. 5B indicates a single fibroblast cell **500**. Both FIG. 5A and FIG. 5B show fibroblast cells **500** in the second layer. Addition of TGF- β increased the number of cells with either fibroblasts or myofibroblasts in the second layer.

FIG. 6A through FIG. 6D show confocal microscopy images of the cell culture at the end of the eighth week, with and without addition of TGF- β . FIG. 6A shows the control group from a top-view, without TGF- β added. FIG. 6B shows the control group from a side-view without TGF- β added. Alternatively, FIG. 6C is a top-view image of the cell culture with TGF- β added to the cell culture. FIG. 6D is a side-view image, showing the cell culture with TGF- β added to the cell culture. As shown between FIGS. 6A through 6D, greater extracellular matrix deposition is observed when TGF- β is added, in comparison to control groups. DAPI (i.e., 4',6-Diamidino-2-Phenylindole, Dihydrochloride) staining of nuclei in the construct shows that the number of cells at the surface of the mesh increased progressively in TGF- β groups, and the groups treated with TGF- β eventually formed a thicker tissue around the mesh.

FIGS. 7A through 7D show SEM images taken after eight weeks, depicting the three layers of tissue tightly enclosing the stainless steel mesh. FIG. 7A shows the endothelial surface layer, the smooth structures **108**, covering the construct in a confluent manner. FIG. 7B shows that after eight weeks, the tissue shows three different cell layers in sequence, **108** is the surface endothelial layer, **106** is the middle fibroblast and myofibroblast layer, and **104** is the base layer of smooth muscle cells. FIG. 7C and FIG. 7D show that the mesh **102** is tightly integrated with the tissue membrane, with FIG. 7C further illustrating that the cells **104** are penetrating through the mesh **102** opening holes. It can be observed that adding the second and the third layers improves production of the ECM (mainly collagen and glycosaminoglycans) that covers the mesh, forming a confluent smooth surface with endothelial cell lining in both experimental groups.

As noted above, the metal mesh is any suitable material that can operate as scaffolding for a tissue. Further, the mesh can be in any form, non-limiting examples of which include being braided or flat (e.g., the mesh is fabricated as sheet of punched wire mesh or with a woven pattern). In another aspect, a Nitinol metal mesh scaffold may be used instead of stainless steel metal mesh for the scaffold. For scale comparison, FIG. 8A shows multiple sheets of one centimeter by one centimeter Nitinol mesh **800** in relation to a United States one cent coin **802**. In production of the tissue, the Nitinol metal mesh **800** is etched with acid in the same process used for the Stainless Steel metal mesh. In this non-limiting example, the mesh **800** is made of a superelastic Nitinol sheet with the thickness of 76 microns etched as a network of holes with 240 microns diameter and the central distance of 320 microns. For the heart valve leaflet application, a sheet that is 25 microns thick is used, which provides the desired elastic recoil of the leaflets. In this aspect, the mesh

800 is cut to the shape of a heart valve leaflet. The Nitinol mesh is seeded with cells in the same manner as the described for the Stainless Steel mesh. An example of the resulting scaffold **100** that is grown for 3 months is shown in FIG. 8B.

As noted above, the scaffold of the present disclosure can be incorporated into any suitable tissue based item, a non-limiting example of which includes a vascular graft. As another non-limiting example and as shown in FIGS. 9A through 9C, the scaffold may be incorporated into a tissue heart valve that mimicks the natural heart valve. The tissue heart valve comprises a flexible frame having a saddle-shaped base **901** and at least two upstanding posts **902** (or three as depicted), which divide the base into at least two portions (or three as depicted), together with tissue leaflets **903** formed from the tissue described in this application. The posts **902** can be formed at opposite ends of a diameter of an undistorted base or, as depicted three (or more) posts **902** are placed at regular intervals around the base.

The tissue leaflets **903** each having a periphery consisting of a free portion **906** extending between the tips of posts **902** and a fixed portion secured, sealed or sutured to corresponding sides of the posts **902** and the adjacent portion of the base **901**. The leaflets **903** are made of a mesh material, such as but not limited to superelastic Nitinol mesh (or Stainless Steel or any other suitable mesh material). The superelastic mesh acts as a structure that defines the shape of the leaflets **903** and can be a structure, such as but not limited to a mesh with arranged or unarranged holes. The mesh can be fabricated, such as but not limited to a sheet of punched wire mesh or with a woven pattern.

To use the heart valve shown in FIGS. 9A through 9C, the saddle-shaped base **901** is attached to the circumference of the auriculoventricular orifice, preferably through an intermediate suture ring **904**, whereby the base can deform from a substantially circular shape to the shape of the orifice simultaneously, as is the case with the natural heart valve. In a valve replacement, the posts **902** may be disposed at regular intervals round the undistorted base, or at other intervals as needed, for example, by the anatomical requirements of coronary ostia in aortic valve replacement.

The flexible frame (i.e., saddle-shaped base **901** and at least two upstanding posts **902**) is formed of any suitably flexible yet durable material. As a non-limiting example, the flexible frame is desirably formed of Elgiloy covered with a woven polyester cloth **912** (such as but not limited to Dacron cloth, or any other suitable covering material), with the differential flexibility afforded by differing thicknesses of the frame material to either side of the posts and/or differing thicknesses of Elgiloy at each portion of the posts. It is designed to be compliant at the orifice and commissures to reduce the closing loading shocks at the commissure tips and free margin of the leaflets. The suture ring **904** can contain inserts of silicone rubber and non-woven polyester. At least two contrasting marking sutures **905** are located on the suture ring **904**. The marking sutures **905** are intended to aid in the proper orientation for implanting the prosthesis. The posts **902** desirably merge at each side into the respective arcuate portions of the saddle-shaped base **901**, with the merging preferably being by way of a continuous curve from the rounded tip of one post **902** to the rounded tip of the other post **902**.

For example in a tri-leaflet valve, the shape of each leaflet **903** preferably corresponds to a portion of a surface of a cone, which portion is defined by the intersections on the conical surface of three flat planes with sixty degree angles together. The three flat panes having peripheries on the

conical surface corresponding in length respectively to the circumference of the saddle-shaped base and the distance between the tips of the posts of the frame. A forth intersection is included on the conical surface of a curved plane that is concave towards the apex of the cone and intersects the three mentioned flat planes at opposite sides of the cone. The spacing of the flat planes and the curvature of the curved plane are such that the development of the curved plane on the conical surface matches in length and curvature a continuously blending of the curve of one arcuate portion of the saddle-shaped base and the adjacent sides of the posts, so that no molding or stress-fixing of the leaflet material is required.

For further understanding of the scaffold nature of the heart valve, FIG. 9A depicts the heart valve with the mesh (such as Nitinol mesh 800) that is the underlying base structure of the leaflets 903. Specifically, FIG. 9A illustrates the heart valve and its scaffold without the biological matrix. FIG. 9A includes an enlarged view 910 of the mesh 800 to illustrate a non-limiting example of a mesh pattern and the holes therethrough. Further, as shown in FIG. 9B, the three layers are grown on top of the Nitinol mesh 800. Specifically, shown is the first layer 104 of smooth muscle cells, the second layer 106 of fibroblast and myofibroblast cells and the third layer 108 of endothelial cells. Finally, FIG. 9C illustrates a resulting heart valve, where the outer layer of each leaflet 903 is the third layer 108 (or endothelial cells).

For further understanding of a suitable base structure, FIG. 9D illustrates components of the heart valve as depicted in FIG. 9A. Shown in FIG. 9D is the flexible frame that includes the saddle-shaped base 901 and at least two upstanding posts 902. The suture ring 904 is also depicted in FIG. 9D, along with the suture material 914. Further, the leaflets 903 are shown, including an enlarged view 910 of the mesh to illustrate an example of the mesh pattern.

As shown, the leaflets 903 can be attached together to form a dimensionally stable and consistent coating leaflet subassembly 916 when subjected to physiological pressures. Then each of the leaflets 903 of the subassembly 916 is aligned with and individually sewn to the frame (i.e., the saddle-shaped base 901 and posts 902), typically from one commissure tip (i.e., post 902), uniformly around the leaflet 903 cusp perimeter, to the tip of an adjacent commissure tip (post 902). The frame (base 901 and 902) is usually covered with cloth but can alternatively be covered with biologic tissue. The sewed sutures 914 act like similarly aligned staples, all of which equally take toe loading force acting along the entire cusp of each of the pre-aligned leaflets 903. The resulting structural assembly (i.e., the heart valve 918 depicted at the top of FIG. 9D and also shown in FIG. 9A) thereby formed reduces stress and potential fatigue at the leaflet suture interface by distributing stress evenly over the entire leaflet cusp from commissure to commissure. Thus, unlike some bioprosthetic valves wherein leaflets are attached individually and the peripheral stitching of the cusps terminates before the tips of the commissures, producing a potential stress point, the produced valve assembly has uniform stitching from commissure tip to commissure tip and consistently aligned coapting leaflet mating edges. This is further illustrated in FIG. 9E, which provides various view-point illustrations of the tri-leaflet heart valve to clearly illustrate the shape of the valve assembly (i.e., tri-leaflet heart valve) and its leaflet mating edges. Finally

and for further illustration, FIG. 9F provides an illustration of the tri-leaflet scaffold that is depicted in FIGS. 9A and 9D.

FIG. 10A and FIG. 10B provide yet another example of a tissue based item that can be adapted or formed to incorporate the scaffold. For example, FIG. 10A is a schematic representation of a blood vessel, depicting the various components of an actual blood vessel. Alternatively, FIG. 10B illustrates the scaffold formed as a blood vessel. As shown, the scaffold in this example includes the base Nitinol mesh 800 that is provided in a tubular wire mesh form to mimic the shape of a blood vessel. The corresponding tissue is grown around the Nitinol mesh 800. Thus, as can be appreciated, the present disclosure enables generation of a variety of scaffolds that are strong enough to resist forces that exist inside a body, while possessing biocompatible surfaces.

Mesh Made Heart Valves

Some embodiments relate to development of a heart valve, whose leaflets are made of a mesh material.

Valvular heart disease is one of the most common causes of heart problems and is associated with high mortality. Treatment for severe cases is valve replacement or valve repair. Over 260,000 replacement procedures are performed each year worldwide. Two types of valves are currently used: mechanical and bioprosthetic (tissue). Mechanical valves are recommended for patients aged 15-64 because they are durable; however, they significantly increase the risk of blood clot formation and require patients to be on lifelong anticoagulation medication, which increases the likelihood of life-threatening bleeding episodes. Bioprosthetic valves, on the other hand, are biocompatible and do not require the use of anticoagulants. However, they last on average only 15-20 years, with 30% of patients requiring reoperation within the first 10 years. This is not as significant for the cohort that is 65 and older, since they have a shorter life expectancy, but is problematic for younger patients because health risks increase with each reoperation. Clearly, there is a need for a valve that solves both the issue of biocompatibility and durability for patients.

In some embodiments, the mesh material is a polymer, such as a surgical mesh. Biocompatibility of polymer mesh implants is good. For example, polyvinylidene fluoride (PVDF, PRONOVA™) is a non-absorbable polymer which features superior textile and biostable properties. Compared to polyester, it shows a higher mechanical stability. In addition, progression of rigidity is not an issue, for example as seen with polypropylene. PVDF is an advantageous alternative to other commonly used materials due to an improved biostability and biocompatibility.

In some embodiments, the mesh material is a thermoplastic polyurethane, such as CARBOTHANE, which is a family of aliphatic and aromatic, polycarbonate-based thermoplastic polyurethanes (TPUs) that are available in a wide range of hardness, color, and radiopacifier formulations. CARBOTHANE TPU has elevated performance properties, such as resistance to bodily fluids and good oxidative and biocompatible properties. Medical-grade TPU are suitable for long term implantation applications. Examples of Aromatic and Aliphatic Polycarbonate-based thermoplastic polyurethanes, e.g., versions marketed by The Lubrizol Corporation, are listed in Tables 1 and 2 below.

TABLE 1

Medical Grade Aromatic Polycarbonate-based thermoplastic polyurethanes:					
Properties	ASTM Test	AC-4075A	AC-4085A	AC-4095A	AC-4055D
Durometer (Shore Hardness)	D785	77A	85A	95A	56D
Specific Gravity	D792	1.19	1.20	1.21	1.22
Ultimate Elongation (%)	D412	8000	9000	10000	11000
Ultimate Tensile (psi)	D412	400	400	370	300
Tensile Modulus (psi) at 100% Elongation	D412	400	875	2125	3300
at 200% Elongation		1025	2100	4750	6700
at 300% Elongation		4400	6200	7700	N/1
Flexural Modulus (psi)	D790	1500	3500	10800	27700
Vicat Temperature (° C.)	D1525	91	73	124	144
Mold Shrinkage (in/in) (1" x .25" x 6" bar)	D955	0.011	0.011	0.009	0.008
Glass transition temperature	DSC	-23	-24	-10	NA

TABLE 2

Medical Grade Aliphatic Polycarbonate-based Thermoplastic Polyurethanes:						
Properties	ASTM Test	PC-3574A	PC-3585A	PC-3595A	PC-3555D	PC-3572D
Durometer (Shore Hardness)	D2240	70A	80A	90A	50D	69D
Specific Gravity	D792	1.15	1.15	1.15	1.15	1.15
Ultimate Elongation (%)	D412	7200	8300	9600	9700	9600
Ultimate Tensile (psi)	D412	600	425	400	325	325
Tensile Modulus (psi) at 100% Elongation	D412	350	600	1050	1750	3500
at 200% Elongation		500	1100	2250	3100	5400
at 300% Elongation		2000	4000	6400	6800	9200
Flexural Modulus (psi)	D790	1600	1470	6400	19300	134000
Vicat Temperature (° C.)	D1525	46	58	62	51	63
Mold Shrinkage (in/in) (1" x .25" x 6" bar)	D955	0.010	0.010	0.010	0.008	0.008
Glass transition temperature	DSC	-29	-27	-25	-25	NA

In some embodiments, the mesh material is a metal, such as but not limited to superelastic Nitinol material. For example, titanium and titanium alloys offer desirable properties, such as relatively low modulus, good fatigue strength, formability, machinability, corrosion resistance, and biocompatibility. Some embodiments may include a stainless steel mesh. Metal mesh materials may optionally contain a combination of biocompatible metals or be used in conjunction with other biomaterials.

As used herein, "biocompatible metal or biocompatible alloy" is defined as individual metals or metal combinations (alloy). An example of a biocompatible metal is pure titanium or pure zirconium with any additional metals less than 1 wt %. Examples of biocompatible alloys include cobalt-chromium-molybdenum, titanium-aluminum-vanadium, nickel-titanium and zirconium-niobium. Other biocompatible alloys may be made from either zirconium or titanium or tantalum or niobium or hafnium or combinations thereof.

Nitinol is a commonly used metal. Nitinol, which is formed by alloying nickel and titanium (~50% Ni), is a shape memory alloy with superelastic properties similar to that of bone, in comparison to stainless steel (another commonly used biomaterial). This property makes nitinol an especially advantageous material for biomedical applications.

In some embodiments, the mesh material has openings or holes that enable capture of circulatory/stationary/migratory cells, and minimize the effect of the metal on in vivo formed tissue natural remodeling. In some embodiments, the hole openings have a diameter (in inches) of about 0.0005, 0.0010, 0.0020, 0.0030, 0.0040, 0.0050, 0.0060, 0.0070, 0.0080, 0.0088, 0.0090, 0.0100, 0.110, 0.0120, 0.0130, 0.0140, 0.0150, 0.0160, 0.0170, 0.0180, 0.0190, or 0.0200.

In some embodiments, the mesh material has a thickness (in inches) of about 0.0004, 0.0005, 0.0006, 0.0007, 0.0008, 0.0009, 0.0010, 0.0015, 0.0020, 0.0025, 0.0030, 0.0035, 0.0040, 0.0045, 0.0050, 0.0055, 0.0060, 0.0065, 0.0070, 0.0075, 0.0080, 0.0085, 0.0090, 0.0095 or 0.0100.

Surprisingly, the inventors have discovered that heart valve leaflets containing these hole dimensions and thickness demonstrate functional properties very similar to native heart valve leaflets, even in the absence of cells growing on the surface of the mesh. Although the heart valve leaflets contain numerous holes that pass through the mesh, the fluid dynamics of a prosthetic heart valve containing such leaflets are comparable to a native heart valve. Moreover, the flexibility of metal meshes having these dimensions minimizes tissue detachment, clotting or excessive tissue growth.

Surface Modification with Bioactive Materials

With respect to the heart valve leaflets disclosed herein, various types of bioactive materials can be used to optimize cell capture, as well as to promote active recruitment and to provide differentiation guidance.

A mesh used in a heart valve leaflet may be modified to contain a molecule that interacts with a cell adhesion molecule. Cell adhesion molecules (CAMs) are proteins located on a cell surface involved in binding with other cells or with the extracellular matrix (ECM) in the process called cell adhesion. Two well-known examples are CD34 and GLYCAM-1. Any molecule that interacts with a cell adhesion molecule may be associated with a mesh, such as but not limited to a CD34 antibody or a GLYCAM-1 antibody. CD34 molecule is a cluster of differentiation molecule present on certain cells within the human body. It is a cell surface glycoprotein and functions as a cell-cell adhesion factor. Glycosylation-dependent cell adhesion molecule-1 (GLYCAM-1) is a proteoglycan ligand expressed on cells. Integrins, which are one of the major classes of receptors within the extracellular matrix (ECM), mediate cell-ECM interactions with collagen, fibrinogen, fibronectin, and vitronectin. Integrins provide essential links between the extracellular environment and the intracellular signalling pathways. Cadherins are homophilic Ca^{2+} -dependent glycoproteins, which link to the actin filament network through specific linking proteins called catenins. Many cell types express combinations of cadherin types. The extracellular domain has major repeats called extracellular cadherin domains (ECD). Selectins are a family of heterophilic CAMs that bind fucosylated carbohydrates, e.g., mucins. Three family members include E-selectin (endothelial), L-selectin (leukocyte), and P-selectin (platelet). A well characterized ligand for the three selectins is P-selectin glycoprotein ligand-1 (PSGL-1), a mucin-type glycoprotein expressed on white blood cells.

A mesh used in a heart valve leaflet may be modified to contain a molecule that interacts with a cellular receptor, such as a growth factor. Epidermal growth factor (EGF) is a growth factor that stimulates cell growth, proliferation, and differentiation by binding to its receptor EGFR. Fibroblast growth factors (FGFs) are a family of growth factors, with members involved in angiogenesis, wound healing, embryonic development and various endocrine signaling pathways. The mammalian fibroblast growth factor receptor family includes FGFR1, FGFR2, FGFR3, and FGFR4. Vascular endothelial growth factor (VEGF) is a signal protein produced by cells that stimulates vasculogenesis and angiogenesis. VEGFs include VEGF-A, VEGF-B, VEGF-C and VEGF-D, and placenta growth factor (PGF).

A mesh used in a heart valve leaflet may be modified to contain a subendothelial extracellular matrix molecule, such as fibulin-5 and fibrillin-1, or an extracellular matrix molecule.

A mesh used in a heart valve leaflet may be modified to contain a peptide-based coating, such as an RGD-peptide. Proteins that contain the Arg-Gly-Asp (RGD) attachment site, together with the integrins that serve as receptors for them, constitute a major recognition system for cell adhesion. The RGD sequence is the cell attachment site of a large number of adhesive extracellular matrix, blood, and cell surface proteins.

In some embodiments, a bioactive material is coated onto the surface of a mesh. Such coating may be carried out by: (a) providing a solution comprising a dissolved protein, (b) contacting the solution with a surface of a mesh, (c) allowing coating of the surface of said mesh with said dissolved

protein, and (d) drying of the coated mesh obtained in step (c). In some embodiments, the mesh is a metal mesh.

Surface coating with a bioactive material may facilitate recruitment and/or binding of cells to the mesh due to an interaction between the bioactive material and various cell types, such as endothelial cells, smooth muscle cells and/or fibroblast/myoblast cells, for example by binding to a surface receptor on the cells.

In some embodiments, growth of cells on the mesh surface, for example, surface endothelialization, can prevent thrombogenicity. Nitinol alloy has been applied widely, due to its shape-memory property and superelastic capability.

When materials are introduced to the body, it is important not only that the material does not damage the body, but also that the environment of the body does not damage the implant. One method that prevents the negative effects resulting from this interaction is called passivation. Passivation is a process that removes corrosive implant elements from the implant-body interface and creates an oxide layer on the surface of the implant. The process can cause biomaterials to be more biocompatible. In some embodiments, a metal mesh surface is plasma coated, for example using a low-temperature plasma deposition technique.

In some embodiments, the surface of the metal mesh may be micropatterned, e.g., with mechanical polishing and/or chemical pickling to prepare surface topographies that enhance cell binding.

The disclosed mechanical valves retain adequate mechanical strength and durability similar to the current mechanical valves and they have excellent hemodynamic performance, no immunogenic, thrombogenic or inflammatory reactions. Therefore, there is no need for anticoagulation medication for the patients who use these types of valve. Moreover, the disclosed valves have the ability of capturing the circulatory/stationary/migratory cells of the body to become biologically active to self-growth, repair and remodel. The ability to capture circulatory/stationary/migratory cells of the body may be enhanced by modifying the surface of the valve leaflets, facilitating growth of a tissue layer on the mesh in a suitable environment (such as the body), so that the mesh may be enclosed by the tissue layer.

Referring to FIG. 11, a bioactive heart valve replacement disclosed herein may comprise a flexible frame, similar to currently available bioprosthetic valves, and at least two upstanding posts, which divide the base into at least two portions, together with the mesh leaflets each having a periphery consisting of a free portion extending between the tips of posts and a fixed portion secured, sealed or sutured to corresponding sides of the posts and the adjacent portion of the base.

Once implanted, the heart valve may activate appropriate signaling cascades for cell recruitment and attachment in order to benefit from the body's natural regenerative ability. Currently available artificial heart valves have the disadvantage of lacking such signaling molecules and cannot offer biological functionality on their surface. Consequently, there has been a lot of research on the functional integration of bioactivity into biomaterials.

The compliance of the valve was tested by using a heart pulsed flow simulator system. The results (FIG. 12) confirmed that the Nitinol mesh sheet, which dominates the mechanical properties of the leaflet material, has stiffness that is appropriate for valve function. This was achieved by using an extra thin superelastic Nitinol mesh (25 microns thickness) and also by proper attachment of the leaflets to the valve stand. The design of the Nitinol mesh leaflets is in a way to reduce the amount of stress applied to cells inside the

blood. The dimensions of holes in the mesh and its thickness were chosen not to have a significant effect on the remodeling of the finally formed tissue. An opening size of about 0.0088", which is almost 10 times larger than the dimension of the circulatory/stationary/migratory cells of the body, minimizes the effect of the metal on the in vivo formed tissue natural remodeling. A higher stiffness mismatch could lead to tissue detachment and immediate clotting or stimulated and excessive tissue growth.

EXAMPLE 1

Biocompatibility and Cell Proliferation Tests on a Polycarbonate-Based Thermoplastic Polyurethane Scaffold for Hybrid Tissue Engineered Heart Valve Applications

Cell adhesion and proliferation of human aortic smooth muscle cells (HASMC), normal human lung fibroblasts (NHLF), and umbilical vein endothelial cells (HUVEC) were examined on a polyurethane scaffold material.

Methods

A thermoplastic polyurethane, Aromatic CARBOTHANE AC-4095A (Lubrizol, Inc.), was used as the substrate material because of its desired mechanical and biocompatibility properties (FIG. 13, 14). We determined that its tensile strength of 68.9 MPa and its elastic modulus of 74.5 MPa are both significantly closer to the values for native aortic valve tissue (2.6 MPa and 15 MPa, respectively) than Nitinol (roughly 1200 MPa and 100 GPa, respectively) and that, by utilizing CARBOTHANE, the physical characteristics of a native heart valve could be emulated more accurately than otherwise possible with Nitinol leaflets.

To produce the CARBOTHANE mesh leaflets, 250 micron-thick sheets of the material were laser cut using a Universal Laser Systems 25 W CO2 laser system. Two-dimensional Solidworks models of the leaflet design were converted into AutoCAD files and imported into the laser cutter program. This program will not run properly unless the AutoCAD files were created from 2-D Solidworks models, and the line thickness in AutoCAD is set to 0 mm. Laser system settings were set to 5% power, 5% speed, and 500 ppi (points per inch) to eliminate any burning or excessive melting of the polymer. Following completion of the laser cutting process, leaflets were viewed under a microscope to confirm that the material did not burn due to prolonged exposure to excessive heat. Any leftover circle cutouts from the mesh may be removed using compressed air.

HASMCs, NHLFs, and HUVECs were each seeded on top of 1 cm² pieces of AC-4095A and incubated for 7 days. Cell adhesion and viability was then tested on both fibronectin-treated and untreated substrate material. Samples were stained using Cell Tracker Red CMTPX and imaged using fluorescence microscopy. To determine proliferation rates, the CARBOTHANE pieces were transferred into a fresh well, and the cells were dissociated using TrypLE Express (1x). Cells were then counted in a Cell Countess machine and the populations were compared to the initial seeding density of 100,000 cells/ml (FIG. 15).

Results

AC-4095A showed positive adhesive properties with HASMCs and NHLFs. The cells' level of elongation was used as a factor to determine their ability to adhere to and survive on the CARBOTHANE material. Both cell types attached and survived when cultured on fibronectin coated and untreated AC-4095A. Cells survived on the substrate for the entire 3-day period of the experiment. Fluorescence imaging confirmed HASMC and NHLF viability on the

polyurethane substrate. HUVECs initially attached to the fibronectin coated substrate, but they began to clump together within 24 hours. Similarly, for untreated AC-4095A, HUVECs showed initial attachment but clumped together and died within 24 hours of seeding. Because of the trilayered structure of valve interstitial tissue, it is not necessary for all three layers to show adhesive ability to the CARBOTHANE surface. It was previously confirmed that a trilayered tissue construct of HASMCs, NHLFs, and HUVECs is possible in culture.

When cultured on CARBOTHANE, HASMCs and NHLFs exhibited cell shape characteristics similar to cells cultured on standard Corning Cell Culture Flasks. Both HASMCs and NHLFs elongated when cultured on both fibronectin-treated and untreated AC-4095A. Cells survived on the substrate for the entire 3-day period of the experiment. Fluorescence imaging confirmed HASMC and NHLF viability on the polyurethane substrate (FIGS. 16A and B). HUVECs initially attached and elongated on the fibronectin-treated substrate, but they began to clump together within 24 hours (FIG. 16C). Similarly, for untreated AC-4095A, HUVECs showed initial attachment but clumped together and died within 24 hours of seeding. Cell proliferation tests confirmed the suggestion that HASMCs and NHLFs exhibit normal growth properties, while HUVECs do not. A significant increase in population for both HASMCs and NHLFs was observed (215,000+55,000 and 490,000+100,000, respectively) (FIG. 15). HUVEC populations decreased significantly (60,000+20,000), likely due to weak adhesive properties of these cells on the CARBOTHANE surface.

Following confirmation of cell survival and proliferation on the CARBOTHANE squares, tri-layered tissue growth on CARBOTHANE mesh was examined. CARBOTHANE sheets were laser cut to create a mesh to allow for the growth of tissue through the scaffold to enhance the strength of the leaflets. HASMCs were suspended in 5 mg/ml collagen type I, and 250,000 cells were pipetted directly on the mesh. The cell-collagen mixture was allowed to polymerize before submerging in cell media and placed in the incubator. Every 24 hours, the mesh samples were flipped and another layer of cells was seeded onto the scaffold. This process was completed two times for each cell type until the tri-layered tissue was fully seeded. Samples were then incubated for seven days, with the cell media mixture changed every 24 hours. Throughout this process, cells continued to elongate and proliferate, which was confirmed by visual inspection under a microscope. Following completion of the tissue growth process, samples were fixed using 4% formaldehyde. The samples were sent out for immunohistochemistry staining and cross-sectioning to determine the success of the tri-layered aspect of the experiment.

The biocompatibility properties of CARBOTHANE AC-4095A were tested using HASMCs, NHLFs, and HUVECs. Each cell type was seeded on fibronectin coated and untreated substrates, and cell attachment and viability were observed using fluorescence microscopy. HASMCs and NHLFs exhibited good attachment and proliferation on both fibronectin coated and untreated substrates, while HUVECs did not attach as well to either substrate. HUVECs began to clump together and die within 24 hours of seeding. However, all three cell types survived during the tri-layered tissue growth experiment. CARBOTHANE AC-4095A is an ideal candidate for hybrid-TEHV scaffold material because of its excellent durability and biocompatibility.

Conclusions

The adhesive properties of CARBOTHANE AC-4095A were tested using HASMCs, NHLFs, and HUVECs. Each

cell type was seeded on fibronectin-treated and untreated substrates, and cell attachment and viability were observed using fluorescence microscopy. HASMCs and NHLFs exhibited normal attachment characteristics on both fibronectin-treated and untreated substrates, while HUVECs did not attach to either substrate long term. HASMCs and NHLFs attached and elongated on CARBOTHANE, but HUVECs began to clump together and die within 24 hours of seeding. Proliferation tests confirmed these results by showing an increase in population of HASMCs and NHLFs but a decrease in population of HUVECs. Because of the trilayered nature of the valve interstitial tissue, thermoplastic polyurethane polymer materials, such as CARBOTHANE AC-4095A, provide a basis for use as a scaffold for hybrid tissue-engineered heart valve leaflets.

EXAMPLE 2

Accelerated Wear Testing (AWT) and Pulsatile Flow Simulator (PFS) of Polymer Valves
Purpose

We tested the use of a thermoplastic polyurethane polymer (Aromatic CARBOTHANE—AC) as a scaffold material for hybrid tissue valves. We report the durability and functionality of the polymer by using Accelerated Wear Testing (AWT) and a Pulsatile Flow Simulator (PFS), pertaining to our hybrid tissue-engineered heart valve. These designs are constructed utilizing AC, which is a biocompatible material. We determined that the design provides improved durability and functionality for the hybrid valve. The valve can be used for culturing cells and collagen. We tested the design using AWT and a PFS machine to investigate the valve durability and functionality.

Scope

Durability and functionality are essential for hybrid tissue valves (HTV's). We designed and built polymer valves using Aromatic CARBOTHANE polymer leaflets and Titanium frames. We measured durability of the valves over 50 million cycles and functionality of the valves by measuring Geometric Orifice Area (GOA).

Background

Mechanical and bioprosthetic valves are the most prevalent types of current heart valves offered for patients in need of an artificial heart valve replacement. Both types of artificial valves as a replacement to a patients' native valve have inherent risks and concerns for patients. Currently there are two basic types of Bioprosthetic heart valves. Tissue valves are manufactured using a biocompatible tissue. A mechanical heart valve is made from materials that do not include any form of biological tissue (pig, cow, horse). Instead, they include very strong materials, such as titanium and carbon. However, current tissue bioprosthetic heart valves have lower durability and are calcified in a shorter time than that of a mechanical valve. Thus, each type of these valves has its own advantages and disadvantages, depending on patient conditions. Thus, there is a need to design and build a novel valve to improve upon the above issues. Recently, the hybrid tissue engineered heart valve offers patients a novel valve. Hybrid tissue valves also help to improve the durability and functionality issues of bioprosthetic valves and they help patients to avoid anticoagulation therapy (J. E. Rossi, "Anticoagulation in TAVR" American College of Cardiology, Mar. 17, 2014).

Test Articles and Controls

The following tools and resources were used:

a) Test Articles: Two valves were manufactured using an AC polymer as a new biocompatible material. Valve con-

struction and materials were identical with one exception. For valve two, each of the three posts were stiffer than those utilized to construct valve one.

b) AWT Simulator: We used an AWT M6 simulator made by the DYNATEK Company. The M6 can test two to six heart valves simultaneously. Our M6 simulator is equipped with two pressure transducers and a thermocouple. The two valves were simultaneously tested for 50 million cycles, with a closing pressure of 120 mm Hg. FIG. 1 shows our M6 simulator under valve durability testing. We used the M6 AWT simulator to measure valve durability over fifty million cycles. The AWT machine can simultaneously run 6 valves at a maximum pressure of 250 mmHg and 1000 cpm. Also, we used our custom PFS simulator to measure valve functionality. The PFS simulator provides a pulsated flow range from 1 to 4.5 liter per minutes. The two valves have been tested using two different pulse rates. (3.6 And 4.4 liter per minutes). FIG. 2 shows our PFS simulator during valve functionality testing.

c) Software: All measurements were done by DYNATEK Labs software for the valve durability data taken from the AWT simulator. Also we use ImageJ software to measure geometric orifice area (GOA) and calculated orifice area (COA) from images taken from the PFS simulator.

d) Controls: This is an investigational study only. We did not run a control group for this study. However, all devices used to measure the variables have been tuned before the valve testing.

e) Statistics: Since the number of tests was limited, no specific method of analysis was used. However, the data measured from both valves has been compared and quantified.

Methodology

a) Image quality: All images were captured by a camera. All images were imported into ImageJ software. All images have been calibrated by the software and calculated orifice areas (COA) were measured for both valves.

b) Phase of study: All measurements were done at 50 million cycles, at 120 mmHg pressure on the AWT simulator. All measurements were done at 3.6 and 4.4 liter per minute in 70 heart beats using our PFS simulator.

c) Variables and method of assessment:

I. Measure of COA: For this variable, we used images taken from PFS simulator. When the valves are in the open and close positions, the areas of opened and closed valve were measured. FIG. 20 shows the calculated area from the valve at opened position.

II. Dimensions of COA: First, pixel measurements were done by the ImageJ software. Then, the data were converted to mm², based on image calibration. FIG. 20 shows an image how we calibrated the image and converted it to mm. The black line shows the inner diameter of PFS tube which is 31.6 mm.

III. Maximum of COA were measured by ImageJ software. The opened area was highlighted by a black line shown in FIG. 19. Then, the area was measured in pixels and was converted to mm based on the calibration picture (FIG. 20). The COA method performed for a both valve at two different flow rates.

IV. Post displacement was measured by ImageJ software. The two images taken from the valve at opened and closed positions were imported into ImageJ software. The location of the post was quantified at both images. Then, the post displacement was calculated based on the location of the post in the images. FIG. 21 shows how the post displacement was calculated. The white line shows the post displacement for the valve in our PFS machine.

V. AWT simulator was set to run for 50 million cycles at 800 cpm and pressure of 120 mmHg. The pressure of inflow and outflow were measured by two pressure transducers. The transducers were calibrated before the test by a transducer tester. The pressure from both transducers were recorded by the DYNATEK software throughout the valve testing (FIG. 22). Also, a stroboscope was used to track the valve at opening and closing positions to monitor the orifice area.

Results:

Both valves were tested by PFS simulator and the COA's were measured at two different flow rates. Table 1 shows the results of COA's in mm².

Valves	Rate L/min	Opened area mm ²
Valve 2	3.6	124.28
Valve 2	4.4	140.36
Valve 1	3.6	93.91
Valve 1	4.4	115.8

Both valves were run by the PFS simulator and the post displacement of both valves were measured at two different flow rates. Table 2 shows the calculated displacement taken from both valves.

Valves	Rate L/min	Displacement mm
Valve 2	3.6	3.685
Valve 2	4.4	5.215
Valve 1	3.6	3.582
Valve 1	4.4	4.385

Both valves first were tested by the AWT simulator and then they were tested by PFS simulator. No damage was found in both valves after 50 million cycles run by the AWT machine. We did not detect any damage on the posts and leaflets on both valves. The valves were run by the AWT at the same time and FIG. 22 shows a short part of the pressure measured by the transducers.

Unexpected Superior Function of a Thermoplastic Polyurethane (TPU) Mesh Material

A common problem with many tissue engineered heart valves is a progressive deterioration that leads to regurgitation and/or leaflet thickening a few months after implantation. The use of bioresorbable scaffolds is speculated to be one factor affecting these valves' failure.

We have previously developed a non-degradable superelastic nitinol mesh scaffold concept that can be used for heart valve tissue engineering applications (Alavi et al. 2011 *Tissue Engineering Part C Methods* 18: 293-301). The use of a non-degradable, superelastic nitinol mesh may increase the durability of tissue engineered heart valves, avoid their shrinkage, and accordingly prevent regurgitation (2017 *Annals of Biomedical Engineering* 45(2): 413-426). However, we discovered that nitinol valve scaffolds, with no flexible posts or no interconnecting fabrics between their leaflets and frames and peripherally meshed nitinol leaflets, showed unfavorable results. We identified three requirements for proper function of the nitinol scaffolds. First, when used with nitinol meshes, the valve frames should be made of a durable material such as titanium with separate stands made of flexible materials, such as PET, to reduce the overall stress over the posts and to enhance opening and closure of the valve's leaflets. Second, the leaflets require a "no-hole" peripheral area at the basal attachment and at their free edges

to avoid leaflet fracture due to excessive stress. Third, the presence of a thin fabric in between the leaflets and frame/stands helps to reduce stress exerted over the leaflets by minimizing leaflet deflection during the valve function. Thus, auxiliary materials and special configurations are required for nitinol-based scaffolds to function properly and to have durability.

In contrast, we unexpectedly discovered that heart valves made from a thermoplastic polyurethane polymer (Aromatic CARBOTHANE-AC) showed excellent function and durability without such limitations. It was surprising that there was no detectable damage on the posts and leaflets on both valves, even after 50 million cycles run by the AWT machine.

Conclusion:

Our results generated from AWT and PFC simulators demonstrate that both valves made from Aromatic CARBOTHANE polymer and a Titanium frame can be opened and closed without issue. Both valves functioned for a total amount of 50 million cycles without any damage throughout the valve testing. The COA calculated from Valve 2 with stiffer posts and longer leaflets shows slightly higher COA and post displacements. We believe that the improvement of valve 2 was due to the stiffer post construction. In spite of providing higher COA and post displacement, the leaflet coaptation lines of Valve 2 do not match one another symmetrically. It is possible that the longer leaflets may provide more flexibility to the valve which leads to the nonsymmetrical coaptation line of leaflets. However, valve 2 has a slightly higher COA and post movement in comparison to valve 1. At the end, our results show that both valves have a good durability and functionality.

EXAMPLE 3

Implantation of Hybrid Valve in Sheep

Purpose

To test the in vivo function, biocompatibility and durability of hybrid valves made from Aromatic CARBOTHANE polymer and Titanium frame.

Methods

The polyurethane core, made from Aromatic CARBOTHANE polymer, was covered by collagen fiber and endothelial cell on both side (aortic side and ventricular side).

A mixture of SMC and fibroblasts used were harvested from a jugular vein of the same sheep. This provides a basis for using pieces of saphenous vein for corresponding use in humans. Since it is not easy to get aortic smooth muscle cells from a human, peripheral vein cells provide a convenient and useful alternative.

Open chest surgery was performed under general anesthesia, and the hybrid valve was implanted in the mitral position.

Results

Abnormal mobility of the valve leaflets was not observed. The leaflets sufficiently opened in echocardiographic images. No apparent regurgitation was observed in the implanted hybrid valve.

Mitral valve replacement was successfully performed and the sheep was able to walk around and drink water after the recovery from anesthesia.

It is understood that the examples and embodiments described herein are for illustrative purposes only and that various modifications or changes in light thereof will be suggested to persons skilled in the art and are to be included within the spirit and purview of this application and scope of any appended claims. All figures, tables, and appendices, as

well as publications, patents, and patent applications, cited herein are hereby incorporated by reference in their entirety for all purposes.

What is claimed is:

1. A heart valve comprising a heart valve leaflet comprising a thermoplastic polyurethane (TPU) mesh material, wherein the thermoplastic polyurethane (TPU) mesh material has a tensile strength and an elastic modulus that are within an order of magnitude from the tensile strength and elastic modulus of native heart valve tissue, and wherein the heart valve withstands at least 50 million cycles of accelerated wear testing (AWT) with no detectable damage on the frame and leaflets.

2. The heart valve according to claim 1 comprising one to three layers of cells cultured on each side of the mesh material.

3. The heart valve according to claim 2, wherein the one to three layers of cells comprise smooth muscle cells, fibroblasts, and/or endothelial cell populations.

4. The heart valve according to claim 3, wherein the smooth muscle cells are vascular smooth muscle cells (VSMC).

5. The heart valve according to claim 2, wherein the one to three layers of cells cultured on each side of the mesh material comprise a first layer of smooth muscle cells formed directly on the thermoplastic polyurethane mesh, a second layer of fibroblast/myofibroblast cells formed on the first layer, and a third layer of endothelial cells formed on the second layer.

6. The heart valve according to claim 2, wherein a first layer of smooth muscle cells and fibroblast/myofibroblast cells are intermixed together and are formed directly on the thermoplastic polyurethane mesh, and a second layer of endothelial cells is formed on the first layer.

7. The heart valve of claim 1, wherein the TPU mesh material comprises an aliphatic polycarbonate-based thermoplastic polyurethane or an aromatic polycarbonate-based thermoplastic polyurethane.

8. The heart valve of claim 1, wherein the thermoplastic polyurethane (TPU) mesh material has a tensile strength of about 68.9 MPa, an elastic modulus of about 74.5 MPa.

9. The heart valve of claim 1, wherein the leaflet has an ability to capture circulatory/stationary/migratory cells of the body to become biologically active.

10. The heart valve of claim 1, wherein the leaflet has a modified surface, which facilitates growth of a tissue layer on the leaflet, such that the mesh may become enclosed in the tissue layer.

11. The heart valve of claim 10, wherein the surface of the leaflet is modified by plasma coating.

12. The heart valve of claim 10, wherein the surface of the mesh is micropatterned to enhance cell binding.

13. The heart valve of claim 1, wherein a bioactive material is used to coat the leaflet to optimize cell capture and/or to actively recruit cells and/or provide cell differentiation guidance.

14. The heart valve of claim 13, wherein the bioactive material is selected from the group consisting of a molecule that binds to a cell adhesion molecule (CAM), a growth factor, an extracellular matrix molecule, a subendothelial extracellular matrix molecule and a peptide.

15. The heart valve of claim 14, wherein the molecule that binds to a CAM is a CD34 antibody.

16. The heart valve of claim 14, wherein the growth factor is selected from the group consisting of epidermal growth factor (EGF), fibroblast growth factor 1 (FGF1), FGF2, FGF3, FGF4, vascular endothelial growth factor-A (VEGF-A), VEGF-B, VEGF-C, VEGF-D, and placental growth factor (PGF).

17. The heart valve of claim 14, wherein the subendothelial extracellular matrix molecule is selected from the group consisting of fibronectin, fibulin-5 and fibrillin-1.

18. The heart valve of claim 14, wherein the peptide is an RGD-peptide.

19. The heart valve of leaflet claim 1, wherein the mesh has a stiffness equivalent to a native heart valve leaflet, such that it functionally mimics a native heart valve leaflet.

20. The heart valve of claim 1, wherein the mesh has a hole diameter of between 0.0005-0.0400 inches.

21. The heart valve of claim 20, wherein the mesh has a hole diameter of about 0.0088 inches.

22. The heart valve of claim 1, wherein the mesh has a thickness of between 0.0004-0.0100 inches.

23. The heart valve of claim 22, wherein the mesh has a thickness of about 0.001 inches.

24. The heart valve according to claim 1, comprising a metal frame.

25. The heart valve according to claim 24, wherein the metal frame comprises titanium.

26. The heart valve according to claim 24, wherein the metal frame is 3D printed.

* * * * *